

Generalized parton distributions and rapidity gap survival in exclusive diffractive pp scattering

L. Frankfurt,¹ C.E. Hyde-Wright,² M. Strikman,³ and C. Weiss⁴

¹*School of Physics and Astronomy, Tel Aviv University, Tel Aviv, Israel*

²*Old Dominion University, Norfolk, VA 23529, USA*

³*Department of Physics, Pennsylvania State University, University Park, PA 16802, USA*

⁴*Theory Center, Jefferson Lab, Newport News, VA 23606, USA*

We propose a new approach to the problem of rapidity gap survival (RGS) in the production of high-mass systems (H = dijet, heavy quarkonium, Higgs boson) in double-gap exclusive diffractive pp scattering, $pp \rightarrow p + (\text{gap}) + H + (\text{gap}) + p$. It is based on the idea that hard and soft interactions proceed over widely different time- and distance scales and are thus approximately independent. The high-mass system is produced in a hard scattering process with exchange of two gluons between the protons. Its amplitude is calculable in terms of the gluon generalized parton distributions (GPDs) in the protons, which can be measured in J/ψ production in exclusive ep scattering. The hard scattering process is modified by soft spectator interactions, which we calculate in a model-independent way in terms of the pp elastic scattering amplitude. Contributions from inelastic intermediate states are suppressed. A simple geometric picture of the interplay of hard and soft interactions in diffraction is obtained. The onset of the black-disk limit in pp scattering at TeV energies strongly suppresses diffraction at small impact parameters and is the main factor in determining the RGS probability. Correlations between hard and soft interactions (*e.g.* due to scattering from the long-range pion field of the proton, or due to possible short-range transverse correlations between partons) further decrease the RGS probability. We also investigate the dependence of the diffractive cross section on the transverse momenta of the final-state protons (“diffraction pattern”). By measuring this dependence one can perform detailed tests of the interplay of hard and soft interactions, and even extract information about the gluon GPD in the proton. Such studies appear to be feasible with the planned forward detectors at the LHC.

PACS numbers: 12.38.-t, 13.85.-t, 13.85.Dz, 14.80.Bn

I. INTRODUCTION

Hard processes in high-energy pp scattering are important both as a laboratory for studying strong interaction dynamics and the parton structure of the proton, and as one of the main tools in the search for new heavy particles. Of particular interest are so-called diffractive processes, in which the produced high-mass system (dijet, heavy particle) is separated from the projectile fragments by large rapidity gaps. Double-gap exclusive processes (*i.e.*, without breakup of the protons)

$$pp \rightarrow p + (\text{gap}) + H + (\text{gap}) + p, \quad (1)$$

are considered as an option for the Higgs boson search at the LHC [1, 2, 3, 4, 5]. Such processes have lower cross section than inclusive double-gap processes (with breakup of one or both protons), but offer better chances for detection, and for determining the mass of the produced particle and possibly even its quantum numbers; see Ref. [5] and references therein. Double-gap exclusive processes (1) also appear to be an effective method for producing heavy quarkonia and investigating their properties.

From the point of view of strong interactions, double-gap exclusive events (1) arise as the result of an interesting interplay of “hard” (involving momentum transfers much larger than the typical hadronic mass scale) and “soft” (momentum transfers of the order of the typical

hadronic mass scale) interactions. The high-mass system is produced in a hard scattering process, involving the exchange of two gluons between the protons. The requirement of the absence of QCD radiation ensures the localization of this process in space and time. This alone, however, is not sufficient to guarantee a diffractive event. One must also require that the soft interactions between the spectator systems do not lead to particle production. This results in a suppression of the cross section as compared to the hard scattering process alone, the so-called rapidity gap survival (RGS) probability. While not directly observable, this quantity plays a central role in the discussion of hard diffractive processes and their use in new particle searches.

Diffractive final states are most favorably produced in scattering at large impact parameters (peripheral scattering), where the chances for the spectator systems not to interact inelastically are large. Conversely, this means that the selection of diffractive events changes the effective impact parameters as compared to inclusive events with the same hard scattering process. This effect is essential for understanding the physical mechanism of RGS. In this sense, RGS is a manifestation of a general quantum-mechanical phenomenon — the postselection of certain initial-state configurations by conditions imposed on the final state [6].

The concept of RGS should also be viewed in the context of QCD factorization for the production of heavy particles in pp scattering [7]. QCD factorization was for-

mally proved for inclusive scattering, $pp \rightarrow H+X$. A crucial element in this is the cancellation of initial-state and final-state QCD radiation. This cancellation becomes incomplete if additional conditions, such as rapidity gaps, are imposed on the hadronic final state. The introduction of the RGS probability can be seen as an attempt to “restore” QCD factorization for diffractive processes at the phenomenological level, in a form analogous to the inclusive case.

In this paper, we propose a new approach to RGS in double-gap exclusive hard diffractive processes. It is based on the idea that hard and soft interactions are approximately independent because they happen over widely different time- and distance scales. We implement this idea in the framework of a partonic description of the proton, along the lines of Gribov’s parton picture of high-energy hadron-hadron scattering [8]. In the approximation where hard and soft interactions are considered to be completely independent, one can regard the hard scattering process as a “local operator” in partonic states, and RGS appears as the “renormalization” of this operator due to soft interactions. At the amplitude level, this leads to an absorption correction to the hard production process due to elastic rescattering; contributions from inelastic intermediate states are suppressed because of the different character of the states accessible in hard and soft interactions. At the cross section level, we recover a simple “geometric” expression for the RGS probability, which was suggested on the basis of heuristic arguments in Refs. [9, 10, 11]. In addition to providing a transparent physical picture of RGS, this expression can readily be evaluated in terms of two phenomenological ingredients, both of which can be probed in independent measurements:

- The gluon generalized parton distribution (GPD) in the proton; more precisely its t -dependence (“two-gluon formfactor”), whose Fourier transform describes the transverse spatial distribution of gluons. Information about it comes from measurements of hard exclusive processes in ep scattering, in particular J/ψ photoproduction (HERA, FNAL).
- The pp elastic scattering amplitude at high energies; in particular its profile function in the impact parameter representation. It is known from fits to $pp/\bar{p}p$ total and elastic cross section data up to the Tevatron energy, and constrained by general arguments (black-disk limit, see below)

The framework provided by our partonic approach to RGS allows us to take into account two basic facts about the dynamics of hard and soft interactions at high energies, which turn out to have a decisive influence on the numerical value of the RGS probability. These are:

- *Small transverse radius of hard interactions.* The radius of the transverse distribution of hard gluons in the proton is significantly smaller than the

transverse radius of soft interactions in high-energy pp collisions (“two-scale picture”). This basic fact explains many qualitative features of hard exclusive diffractive processes, such as the effective impact parameters in diffractive events, the order-of-magnitude of the RGS probability, and the pattern of the transverse momentum dependence of the cross section.

- *Black-disk limit in high-energy pp scattering.* Parametrizations of the data as well as general theoretical arguments indicate that the profile function of pp elastic scattering becomes “black” at small impact parameters at energies above the Tevatron energy, $\sqrt{s} > 2\text{TeV}$. This circumstance makes the description of pp scattering at small impact parameters at LHC energies practically model-independent, and is essential for the stability of numerical predictions for the RGS.

The evidence supporting these statements is described in detail in Ref. [9], and summarized in Sections II and III below.

Our partonic approach also allows us to describe the effects of correlations between hard and soft interactions on the RGS probability. Such correlations can arise from various dynamical mechanisms, *e.g.* from the long-range pion field of the proton, or from possible short-range transverse correlations between hard partons, as suggested by the Tevatron CDF data on inclusive pp scattering with multiple hard processes [12]. We find that the inclusion of such correlations decreases the RGS probability compared to the independent interaction approximation. While these effects cannot be calculated in a completely model-independent way, they are important both for our general understanding of the mechanism of RGS, and for obtaining reliable numerical estimates of the RGS probability. These effects clearly merit further study.

A unique feature of exclusive diffractive processes is that the interplay of hard and soft interactions can be studied experimentally, by measuring the dependence of the cross section on the transverse momenta of the final-state protons. The modification of the hard scattering amplitude by soft elastic rescattering can be viewed as an interference phenomenon, which gives rise to a distinctive “diffraction pattern” in the final-state transverse momenta. By measuring this dependence in exclusive diffractive processes with relatively large cross section, such as dijet production, one can perform a variety of tests of the diffractive reaction mechanism, and extract information about the transverse radii of hard and soft interactions and their energy dependence. In Higgs production, measurements of the transverse momentum dependence would allow one to obtain additional information about the parity of the produced particle [5]. Experimentally, such studies appear to be feasible with the planned forward detectors at the LHC [13] and the Tevatron [14].

Detailed studies of RGS in diffractive pp scattering were done in a model of soft interactions based on eikonized Pomeron exchange [4, 5]. We show here that, in the approximation where hard and soft interactions are considered to be independent, the RGS probability unambiguously follows from QCD and can be calculated in a model-independent way. Nevertheless, our numerical results for the RGS probability in this approximation turn out to be of the same order of magnitude as those reported in Refs. [4, 5], which can be attributed to the fact that the Pomeron parametrization of the pp elastic amplitude reproduces the approach to the BDL at small impact parameters. The agreement between our numerical results and theirs at the quantitative level is somewhat accidental, being due to the fact that in the calculation of Refs. [4, 5] the effect from inelastic intermediate states (which in our approach are seen to be strongly suppressed because of the small overlap of states accessible via hard and soft interactions) is partly compensated by the choice of a larger value of the t -slope of the gluon GPD; see Section V for details. Finally, our partonic approach can naturally be extended to include correlations between hard and soft interactions, which have a potentially large numerical effect on the RGS probability.

This paper is organized as follows. In Section II we review the information about the transverse structure of soft interactions from pp elastic scattering, and the approach to the black-disk limit at central impact parameters. In Section III we discuss the properties of the proton's gluon GPD at small x and summarize our knowledge of the transverse spatial distribution of hard partons in the proton. Section IV describes the basic framework of our approach to RGS. We outline the properties of the hard scattering amplitude, describe the theoretical formulation of the independence of hard and soft interactions, and obtain a master expression for the diffractive amplitude combining hard and soft interactions. We then explain the suppression of inelastic intermediate states, and evaluate the diffractive amplitude in terms of the gluon GPD and the pp elastic amplitude. In Section V we use our result for the amplitude in the independent interaction approximation to calculate the RGS probability. We recover a simple geometric expression for the RGS probability and discuss the effective impact parameters in exclusive diffraction. We then evaluate the RGS probability numerically, estimate the uncertainty of the numerical predictions due to the phenomenological input, and emphasize the crucial role of the black-disk limit in stabilizing the numerical predictions. We also comment on the results for the RGS obtained within the eikonized Pomeron model for soft interactions [4] from the perspective of our approach. In Section VI we discuss various effects beyond the approximation of independence hard and soft interactions in exclusive diffraction. We first point out that hard screening corrections may reduce the diffractive cross section beyond the RGS probability due to soft interactions. We then discuss the effect of correlations between hard and soft interactions on the

RGS probability, considering two specific mechanisms — diffractive scattering from the long-range pion field, and short-range transverse correlations between partons. In Section VII we work out the dependence of the exclusive diffractive cross section on the final proton transverse momenta. We discuss which experimentally observable features of this dependence furnish useful tests of the diffractive reaction mechanism, and how one can extract information about the gluon GPD. In Section VIII we summarize our results. We comment on the implications for the Higgs boson search, and on the experimental feasibility of measuring the transverse momentum dependence of exclusive diffraction with the planned forward detectors at the LHC.

II. BLACK-DISK LIMIT IN pp ELASTIC SCATTERING

Information on the transverse radius of strong interactions at high energies comes mostly from measurements of the t -dependence of the differential cross section for pp and $p\bar{p}$ elastic scattering. Combining these data with those on the $pp/\bar{p}p$ total cross section, and implementing theoretical constraints following from the unitarity of the S -matrix, one can reconstruct the complex pp elastic scattering amplitude, $T_{\text{el}}(s, t)$; see *e.g.* Refs. [15, 16, 17]. At high energies, $s \gg |t|$, angular momentum conservation in the CM frame implies that the scattering amplitude is effectively diagonal in the impact parameter of the colliding pp system. It is convenient to represent it as a Fourier integral over a transverse coordinate variable, \mathbf{b} ,

$$T_{\text{el}}(s, t = -\Delta_{\perp}^2) = \frac{is}{4\pi} \int d^2b e^{-i(\Delta_{\perp} \cdot \mathbf{b})} \Gamma(s, \mathbf{b}), \quad (2)$$

where Γ is the (dimensionless) profile function. One can then express the elastic, total, and inelastic (total minus elastic) pp cross sections in terms of the profile function as

$$\left. \begin{aligned} \sigma_{\text{el}}(s) \\ \sigma_{\text{tot}}(s) \\ \sigma_{\text{inel}}(s) \end{aligned} \right\} = \int d^2b \times \left\{ \begin{aligned} &|\Gamma(s, \mathbf{b})|^2, \\ &2 \text{Re} \Gamma(s, \mathbf{b}), \\ &[1 - |1 - \Gamma(s, \mathbf{b})|^2] . \end{aligned} \right. \quad (3)$$

The functions on the R.H.S. describe the distribution of the respective cross sections over pp impact parameters, $b \equiv |\mathbf{b}|$ [60]. In particular, we note that the combination

$$|1 - \Gamma(s, \mathbf{b})|^2 \quad (4)$$

can be interpreted as the probability for “no inelastic interaction” in a pp collision at impact parameter b ; this combination plays an important role in our calculation of the RGS probability (see Section V below) [61]. A measure of the transverse size of the proton is the logarithmic t -slope of the elastic pp cross section at $t = 0$,

$$B \equiv \frac{d}{dt} \left[\frac{d\sigma_{\text{el}}/dt(t)}{d\sigma_{\text{el}}/dt(0)} \right]_{t=0}. \quad (5)$$

At high energies, where the elastic amplitude is predominantly imaginary, and Γ is real, B is equal to half the average squared impact parameter in the total pp cross section,

$$B \approx \frac{\langle b^2 \rangle_{\text{tot}}}{2} \equiv \frac{1}{2} \frac{\int d^2b b^2 2 \text{Re} \Gamma(s, \mathbf{b})}{\int d^2b 2 \text{Re} \Gamma(s, \mathbf{b})}, \quad (6)$$

which may be associated with the transverse area of the individual protons. The data show that the slope increases with the CM energy as

$$B(s) = B(s_0) + 2\alpha' \ln(s/s_0), \quad (7)$$

where $\alpha' \approx 0.25 \text{ GeV}^{-2}$. In the Pomeron exchange parametrization of the pp elastic amplitude this constant is identified with the slope of the Pomeron trajectory.

In Gribov's parton picture of high-energy hadron-hadron interactions [8], the transverse size of the proton in pp elastic scattering can be directly associated with the average transverse radius squared of the distribution of soft partons mediating the soft interactions,

$$B = \langle \rho^2 \rangle_{\text{soft}}. \quad (8)$$

Here and in the following, we use $\rho \equiv |\boldsymbol{\rho}|$ to denote the transverse distance of partons from the center of the proton, and $b = |\mathbf{b}|$ for the impact parameter of the pp collision. The growth of the proton's transverse size with energy is explained as the result of random transverse displacements in the successive decays generating the distribution of soft partons (Gribov diffusion). Below we shall compare this distribution of soft partons to the distribution of hard partons probed in hard exclusive processes (see Section III).

Parametrizations of the available data indicate that at energies above the Tevatron energy, $\sqrt{s} \gtrsim \sqrt{s_{\text{Tevatron}}} = 2 \text{ TeV}$, the profile function at small impact parameters approaches

$$\Gamma(s, b) \rightarrow 1 \quad \text{for } b < b_0(s). \quad (9)$$

This corresponds to unit probability for inelastic scattering for impact parameters $b < b_0(s)$, *cf.* Eqs. (3) and (4), similar to the scattering of a pointlike object from a black disk of radius b_0 , and is referred to as the black-disk limit (BDL) [9, 11, 18].

The approach to the BDL in central pp scattering at high energies is a general prediction of QCD, independent of detailed assumptions about the dynamics. Studies of the interaction of small-size color dipoles with hadrons, based on QCD factorization in the leading $\log Q^2$ approximation, show that the BDL is attained at high energies as a result of the growth of the gluon density at small x due to DGLAP evolution [18]. This result can be used to estimate the interaction of leading projectile partons with the small- x gluons in the target in pp scattering; one finds that there is no chance for the projectile wavefunction to remain coherent in small impact parameter scattering at TeV energies [9, 11]. Similar reasoning allows one to

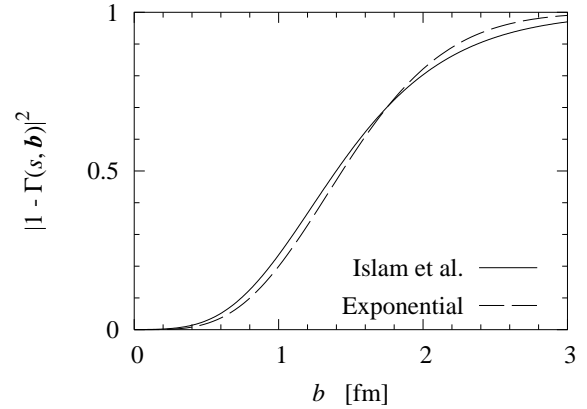


FIG. 1: The probability distribution for no inelastic interaction, $|1 - \Gamma(s, \mathbf{b})|^2$, Eq. (4), as a function of $b \equiv |\mathbf{b}|$, at the LHC energy ($\sqrt{s} = 14 \text{ TeV}$), as computed with different parametrizations of the pp elastic scattering amplitude. Solid line: Parametrization of Islam *et al.* [17] (“diffractive part” only). Dashed line: Exponential parametrization, Eq. (12), with $\Gamma_0 = 1$ (BDL), *cf.* Eq. (14), and $B = 21.8 \text{ GeV}^{-2}$.

predict the growth of the size of the black region, b_0 , with s [9, 11]. As a by-product, these arguments explain why the observed coefficient in the Froissart formula for the total cross sections is significantly smaller than that derived from the general principles of analyticity of the amplitude in momentum transfer and unitarity of the S -matrix [19]. We note that the need for the approach to the BDL in high-energy scattering at central impact parameters was understood already in the pre-QCD period within the Pomeron calculus, where it was noted that this phenomenon resolves the apparent contradiction between the formulae of the triple-Pomeron limit and the unitarity of the S -matrix, especially in models where the Pomeron intercept, $\alpha_P(0)$, exceeds unity [20].

For our studies of diffractive pp scattering it will be useful to have a simple analytic parametrization of the pp elastic amplitude at the LHC energy, which incorporates the approach to the BDL at small impact parameters. The t -dependence of the pp elastic scattering cross section for $|t| \lesssim 1 \text{ GeV}^2$ over the measured energy range is reasonably described by an exponential shape,

$$\frac{d\sigma_{\text{el}}}{dt} \propto \exp[B(s)t], \quad (10)$$

where $B(s)$ represents an effective slope, to be distinguished from the “exact” slope at $t = 0$, Eq. (5). A parametrization of the pp elastic amplitude which reproduces this dependence is

$$T_{\text{el}}(s, t) = \frac{is}{8\pi} \sigma_{\text{tot}}(s) \exp\left[\frac{B(s)t}{2}\right], \quad (11)$$

corresponding to

$$\Gamma(s, \mathbf{b}) = \Gamma_0(s) \exp\left[-\frac{b^2}{2B(s)}\right] \quad (12)$$

with

$$\Gamma_0(s) \equiv \Gamma(s, \mathbf{b} = 0) = \frac{\sigma_{\text{tot}}(s)}{4\pi B(s)}. \quad (13)$$

Equation (11) takes into account that the amplitude at high energies is predominantly imaginary, and satisfies the optical theorem for the total cross section, $\sigma_{\text{tot}}(s) = (8\pi/s) \text{Im} T_{\text{el}}(s, t = 0)$. We may now incorporate the constraint of the BDL at small impact parameters by replacing

$$\Gamma_0 \rightarrow 1. \quad (14)$$

The value of B we determine by comparing the profile function (12) with phenomenological parametrizations of the data, extrapolated to the LHC energy, which gives

$$B \approx 20 \text{ GeV}^{-2} \quad (\sqrt{s} = 14 \text{ TeV}). \quad (15)$$

In particular, with $B = 21.8 \text{ GeV}^{-2}$ we obtain excellent agreement with the Regge parametrization of Ref. [4]. Figure 1 shows the probability for no inelastic interaction, $|1 - \Gamma(s, \mathbf{b})|^2$, Eq. (4), computed with the phenomenological parametrization of Ref. [17] and our exponential parametrization incorporating the BDL, Eqs. (12) and (14). One sees that the simple exponential parametrization is a reasonable overall approximation to the phenomenological parametrization over the b -range shown in Fig. 1.

III. TRANSVERSE SPATIAL DISTRIBUTION OF GLUONS

Information about the transverse structure of hard interactions comes from studies of hard exclusive processes in ep scattering, such as meson electroproduction or virtual Compton scattering. Such processes probe the GPDs in the proton, whose Fourier transform with respect to the transverse momentum transfer to the proton describes the spatial distribution of quarks and gluons in the transverse plane; see Refs. [21, 22] for a review. In this section we summarize what is known about the gluon GPD at small x from theoretical considerations, and from measurements of J/ψ photoproduction and other processes at HERA and in fixed-target experiments.

The gluon GPD can be formally defined as the transition matrix element of the twist-2 QCD gluon operator between proton states of different momenta, p and p' . Physically, it describes the amplitude for a fast-moving proton to “emit” and “absorb” a gluon with given longitudinal momenta, with transverse momenta (virtualities) integrated over up to some hard scale, Q^2 , and a certain invariant momentum transfer to the proton, $t \equiv (p' - p)^2$. The choice of longitudinal momentum variables is a matter of convention. Instead of the initial and final gluon momentum fractions (with respect to the initial proton momentum), x and x' , we use as independent variables the initial gluon momentum fraction, x , and the

fractional longitudinal momentum transfer to the proton (“skewness”) [62]

$$\xi \equiv x - x', \quad (16)$$

and denote the gluon GPD by

$$H_g(x, \xi, t; Q^2). \quad (17)$$

In the limit of zero momentum transfer, the gluon GPD reduces to the usual gluon momentum density in the proton [63]

$$H_g(x, \xi = 0, t = 0; Q^2) = xG(x, Q^2). \quad (18)$$

For discussing the t -dependence of the gluon GPD it is convenient to write it in the form

$$H_g(x, \xi, t; Q^2) = H_g(x, \xi, t = 0; Q^2) F_g(x, \xi, t; Q^2), \quad (19)$$

where the function F_g is known as the “two-gluon formfactor” of the proton and satisfies $F_g(t = 0) = 1$. Note that the two-gluon formfactor still depends on x and ξ , *i.e.*, Eq. (19) does not imply naive factorization of the t -dependence from that on the partonic variables.

The dependence of the gluon GPD on the QCD scale, Q^2 , is governed by the QCD evolution equations. In applications to production of fixed-mass systems in high-energy ep or pp collisions with $M^2 \ll s$ (such as Higgs boson production at the LHC) we shall be interested in the gluon GPD in the region where

$$x, x' \ll 1, \quad (20)$$

while at the same time Q^2 is much larger than the typical hadronic mass scale, $Q^2 \gg 1 \text{ GeV}^2$. In this region the gluon GPD can be calculated by applying QCD evolution to a “primordial” distribution at a low scale, Q_0^2 , in which one neglects the skewness, $\xi = 0$, or $x = x'$ (diagonal approximation) [23, 24]. QCD evolution degrades the individual gluon momentum fractions with increasing Q^2 , while their difference, $\xi = x - x'$, remains fixed by kinematics, being equal to the longitudinal momentum transfer to the proton; as a result, the primordial GPD at the low scale is sampled in the region $|x - x'| \ll x, x'$, where the diagonal approximation is justified. In the diagonal approximation, the GPD at $t = 0$ is completely determined by the usual gluon density, *cf.* Eq. (18), leaving only the t -dependence (two-gluon formfactor) and its correlation with x up to modeling. This approximation makes for a great simplification in applying GPDs at small x , and has been used extensively in the analysis of exclusive electroproduction processes; see Ref. [9] for a review.

For $x \ll 1$, the two-gluon formfactor permits a simple interpretation in terms of a spatial distribution of gluons in the proton. For $\xi \ll 1$, the invariant momentum transfer is dominated by the transverse momentum transfer between the proton states,

$$t \approx -\Delta_\perp^2, \quad \Delta_\perp \equiv \mathbf{p}'_\perp - \mathbf{p}_\perp. \quad (21)$$

The two-gluon formfactor can be represented as a Fourier integral over a transverse coordinate variable, $\boldsymbol{\rho}$,

$$F_g(x, \xi, t = -\Delta_\perp^2; Q^2) = \int d^2\rho e^{-i(\Delta_\perp \rho)} \times F_g(x, \xi, \boldsymbol{\rho}; Q^2). \quad (22)$$

For economy of notation we use the same symbol for the two-gluon formfactor and its Fourier transform, distinguishing the two functions by their arguments. The $\boldsymbol{\rho}$ -dependent function describes the spatial distribution of gluons in the proton in the transverse plane; see Ref. [25] for a review. For $\xi = 0$ (*i.e.*, $x' = x$) it is positive definite and can be interpreted probabilistically as the gluon density at transverse position $\boldsymbol{\rho}$ [26]; for $\xi \neq 0$ it describes the non-diagonal transition matrix element of the gluon density [27]. A measure of the gluonic transverse size of the nucleon for given x and Q^2 is the average of ρ^2 , which is proportional to the t -slope of the two-gluon formfactor at $t = 0$,

$$\langle \rho^2 \rangle_g(x, Q^2) \equiv \int d^2\rho \rho^2 F_g(x, \xi = 0, \boldsymbol{\rho}; Q^2) \quad (23)$$

$$= 4 \frac{\partial F_g}{\partial t}(x, \xi = 0, t = 0; Q^2). \quad (24)$$

The two-gluon formfactor of the nucleon, and hence the transverse spatial distribution of gluons, can directly be extracted from the t -dependence of the differential cross section for hard exclusive vector meson production processes probing the gluon GPD. QCD factorization implies that the t -dependence of the cross section resides solely in the gluon GPD,

$$\left(\frac{d\sigma}{dt} \right)^{\gamma^* p \rightarrow V p} \propto F_g^2(x, \xi, t; Q^2), \quad (25)$$

up to small higher-twist corrections due to the finite size of the produced vector meson [9]. In particular, the t -slope at $t = 0$ is proportional to the proton's average gluonic transverse size,

$$B_g \equiv \frac{d}{dt} \left[\frac{d\sigma/dt(t)}{d\sigma/dt(0)} \right]_{t=0}^{\gamma^* p \rightarrow V p} = \frac{\langle \rho^2 \rangle_g}{2}. \quad (26)$$

A crucial test of the applicability of QCD factorization is provided by the observed convergence of the t -slopes of various gluon-dominated vector meson production processes ($J/\psi, \rho, \phi$) at large Q^2 ; see Ref. [9] for a detailed discussion.

A particularly clean probe of the two-gluon formfactor is J/ψ photoproduction, the t -dependence of which has been measured in experiments at the HERA collider ($x \sim 10^{-2} - 10^{-4}$) [29, 30], the FNAL fixed-target experiment ($\langle x \rangle \sim 5 \times 10^{-2}$) [28], and a number of fixed-target experiments at lower energies ($x \sim 10^{-1}$); see Refs. [31, 32] for a review of the data. This process probes the two-gluon formfactor at an effective scale $Q^2 \approx 3 \text{ GeV}^2$. Analysis of the data, combined with theoretical investigations, has produced a rather detailed

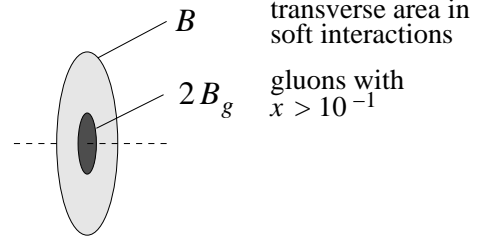


FIG. 2: The “two-scale picture” of the transverse structure of the proton in high-energy collisions.

picture of the gluonic transverse size of the nucleon and its x -dependence [9]. For $x \sim 0.1 - 0.3$, the gluonic transverse size suggested by the fixed-target data is $\langle \rho^2 \rangle_g \approx 0.25 \text{ fm}^2$, close to 2/3 times the proton's axial charge radius, $\langle r^2 \rangle_A$. Between $x \sim 10^{-1}$ and $x \sim 10^{-2}$, $\langle \rho^2 \rangle_g$ increases by $\sim 30\%$. This can be explained by the contribution of the nucleon's pion cloud to the gluon density at large transverse distances, $\rho \sim 1/(2M_\pi)$, which is dynamically suppressed for $x > M_\pi/M_N$ and reaches its full strength for $x \ll M_\pi/M_N$ [33]. Finally, over the HERA range, $x \sim 10^{-2} - 10^{-4}$, the gluonic transverse size exhibits a logarithmic growth with $1/x$,

$$\langle \rho^2 \rangle_g = \langle \rho^2 \rangle_g(x_0) + 4\alpha'_g \ln \frac{x_0}{x} \quad (x < x_0 \approx 10^{-2}), \quad (27)$$

with a rate, α'_g , considerably smaller than that governing the growth of the proton's transverse size in pp elastic scattering, which is dominated by soft interactions,

$$\alpha'_g \ll \alpha'. \quad (28)$$

A recent analysis of the H1 data finds $\alpha'_g = 0.164 \pm 0.028(\text{stat}) \pm 0.030(\text{syst}) \text{ GeV}^{-2}$ for J/ψ photoproduction and $0.019 \pm 0.139(\text{stat}) \pm 0.076(\text{syst}) \text{ GeV}^{-2}$ for electroproduction [29]; an analysis of ZEUS electroproduction data quotes $\alpha'_g = 0.07 \pm 0.05(\text{stat})^{+0.03}_{-0.04}(\text{syst}) \text{ GeV}^{-2}$ [30], significantly smaller than the soft value $\alpha' = 0.25 \text{ GeV}^{-2}$. The smaller rate of growth of the nucleon's size in hard interactions can qualitatively be explained by the suppression of Gribov diffusion in the decay of hard (highly virtual) partons as compared to soft partons.

A crucial observation is that the transverse area occupied by partons with $x \gtrsim 10^{-1}$ is much smaller than the transverse area associated with the proton in soft interactions (see Fig. 2),

$$\langle \rho^2 \rangle_g(x \gtrsim 10^{-1}) \ll \langle \rho^2 \rangle_{\text{soft}}, \quad (29)$$

or

$$2B_g \ll B. \quad (30)$$

In high-energy pp collisions with hard partonic processes one is thus dealing with a two-scale picture of the transverse structure of the proton. Moreover, when considering the production of a heavy particle with fixed mass,

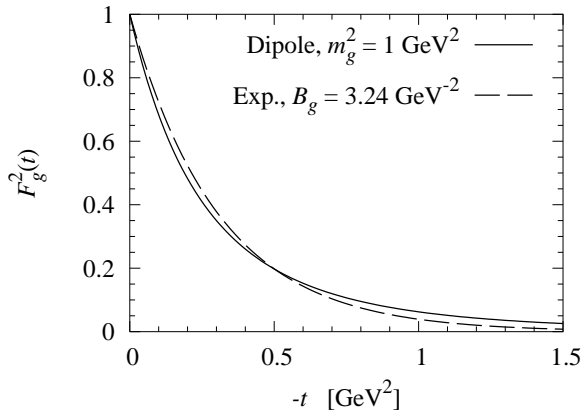


FIG. 3: Comparison of the dipole (solid line) and exponential (dashed line) parametrizations of the two-gluon formfactor, with the parameters related by Eq. (35). Shown is the squared two-gluon formfactor, $F_g^2(t)$, for both parametrizations, as corresponds to the t -dependence of the cross section for J/ψ photoproduction (details see text).

m_H , in a partonic process with $x_{1,2} \sim m_H/\sqrt{s}$, the “soft” area of the proton increases with s faster than the “hard” area (which changes as a result of the decrease of x), because $\alpha' > \alpha'_g$, cf. Eq. (28). Thus, the difference of the two areas becomes even more pronounced with increasing energy.

For our studies of hard processes in diffractive pp scattering we require a parametrization of the t -dependence of the two-gluon formfactor, *viz.* the shape of the transverse spatial distribution of gluons. The x -values probed in Higgs production at central rapidities are $x \sim 10^{-2}$ at the LHC energy. Taking into account the effect of DGLAP evolution, even larger values of x are probed when parametrizing the two-gluon formfactor at the J/ψ production scale, $Q^2 \sim 3 \text{ GeV}^2$ (for a general discussion of the effect of DGLAP evolution on the transverse spatial distribution of gluons, see Ref. [18]). We thus need to look at the J/ψ photoproduction data at $x \gtrsim 10^{-2}$, which are probed in fixed-target experiments.

Theoretical arguments suggest that the two-gluon formfactor at $x \gtrsim 10^{-1}$ should be close to the axial formfactor, which is well described by a dipole form (we omit all arguments except t),

$$F_g(t) = \frac{1}{(1 - t/m_g^2)^2}, \quad (31)$$

with $m_g^2 \approx 1 \text{ GeV}^2$ [31]. The corresponding transverse spatial distribution of gluons is given by

$$F_g(\rho) = \frac{m_g^2}{2\pi} \left(\frac{m_g \rho}{2} \right) K_1(m_g \rho). \quad (32)$$

We also consider an exponential parametrization of the two-gluon formfactor,

$$F_g(t) = \exp(B_g t/2), \quad (33)$$

corresponding to

$$F_g(\rho) = \frac{\exp[-\rho^2/(2B_g)]}{2\pi B_g}. \quad (34)$$

The relation between the parameters of the dipole and exponential parametrization which would follow from identifying $\langle \rho^2 \rangle = 4 dF_g/dt(t=0)$ is $B_g = 4/m_g^2$. Better overall agreement between the squared formfactors for $|t| < 1 \text{ GeV}^2$ is obtained for somewhat smaller values of B_g . Matching the squared formfactors at $|t| = 0.5 \text{ GeV}^2$ we obtain

$$B_g = \frac{3.24}{m_g^2}, \quad (35)$$

see Figure 3. It was shown in Ref. [32] that both the dipole with $m_g^2 = 1.1 \text{ GeV}^2$ and the exponential with $B_g = 3.0 \text{ GeV}^2$ given by Eq. (35) describe well the t -dependence of the data from the FNAL E401/E458 experiment at $\langle E_\gamma \rangle = 100 \text{ GeV}$ in which the recoiling proton was detected [28]. We also note that this value of B_g is consistent with what one obtains from the extrapolation of the HERA data towards larger x , using Eq. (27) with the measured α'_g . We shall use the dipole, Eqs. (31), with $m_g^2 = 1 \text{ GeV}^2$ and the exponential, Eq. (33), with $B_g = 3.24 \text{ GeV}^2$, as our standard parametrizations for calculations in the kinematics of Higgs production at the LHC below; comparison between the two will allow us to estimate the uncertainty of our numerical predictions with respect to the shape of the two-gluon formfactor.

IV. THEORY OF RAPIDITY GAP SURVIVAL

We now outline the basic steps in the calculation of the amplitude of double-gap exclusive diffractive processes (1), and develop the physical picture of RGS. The underlying idea of our approach is that hard and soft interactions are approximately independent, because they happen over widely different distance- and time scales.

A. Hard scattering process

In the first step, one calculates the amplitude for double-gap diffractive production of the high-mass system due to hard interactions. For definiteness, we shall refer in the following to Higgs boson production, keeping in mind that the discussed mechanism applies to production of other high-mass states as well (dijets, heavy quarkonia, *etc.*). According to electroweak theory, the Higgs boson is produced predominantly through its coupling to gluons via a quark loop; for a review and references see Ref. [34]. In contrast to inclusive production, the amplitude for double-gap diffractive production is in the lowest order in the QCD running coupling constant, α_s , given by the exchange of two gluons with

vacuum quantum numbers in the t -channel (see Fig. 4). The Higgs boson is radiated from one of the gluon lines. The role of the second exchanged gluon is to neutralize the color charge in order to avoid gluon bremsstrahlung. However, global color neutrality alone is not sufficient. To suppress radiation, one must require that color be screened locally in space-time. Conversely, this means that the selection of a diffractive process, without accompanying radiation, guarantees some degree of localization of the exchanged system.

Operationally, the localization of the exchanged two-gluon system is ensured by Sudakov formfactors, which suppress configurations with low virtualities prone to emit gluon bremsstrahlung. The actual calculation of the hard scattering amplitude including Sudakov suppression is a challenging problem, which was addressed in various approximations in Refs. [35, 36]. Fortunately, for our purposes we do not need to solve this problem at a fully quantitative level, as only a few qualitative aspects of the hard scattering process turn out to be essential for the physics of RGS.

To discuss the hard scattering process, it is natural to perform a Sudakov decomposition of the four-momenta, using the initial proton momenta, p_1 and p_2 , as basis vectors, with $2(p_1 p_2) = s$ (we neglect the proton mass). As the transverse momenta of the final-state protons are small compared to the Higgs mass, we can expand the final proton four-momenta as

$$\begin{aligned} p'_1 &= (1 - \xi_1)p_1 + p'_{1\perp}, \\ p'_2 &= (1 - \xi_2)p_2 + p'_{2\perp}, \end{aligned} \quad (36)$$

where $(p'_{1\perp}, p_1) = (p'_{1\perp}, p_2) = 0$ etc., and $\xi_{1,2}$ parametrize the longitudinal momentum loss [cf. Eq. (16) and the footnote before it],

$$\xi_{1,2} = \frac{m_H}{\sqrt{s}} e^{\pm y}, \quad (37)$$

where y is the rapidity of the produced Higgs boson. Assuming a Higgs mass of the order of 100 – 200 GeV, the typical values of $\xi_{1,2}$ are of the order of 10^{-2} for production at central rapidities at the LHC ($\sqrt{s} = 14$ TeV).

Consider now the two-gluon exchange process of Fig. 4 as a Feynman diagram, in which the upper and lower blobs denote the gluon-proton scattering amplitudes, to be specified in more detail below. The four-momenta of the gluons coupling to the Higgs we parametrize as

$$k_1 = x_1 p_1 + x'_2 p_2 + k_\perp - p'_{1\perp}, \quad (38)$$

$$k_2 = x'_1 p_1 + x_2 p_2 - k_\perp - p'_{2\perp}. \quad (39)$$

The four-momentum of the screening gluon then follows from four-momentum conservation,

$$k = x'_1 p_1 + x'_2 p_2 + k_\perp, \quad (40)$$

where

$$x'_1 \equiv \xi_1 - x_1, \quad (41)$$

$$x'_2 \equiv \xi_2 + x_2. \quad (42)$$

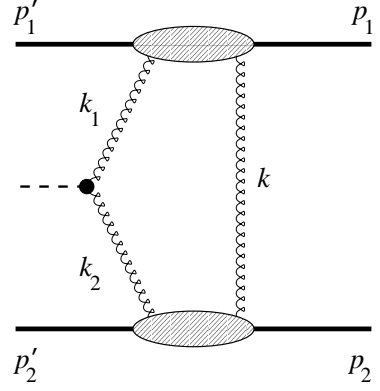


FIG. 4: The hard scattering process in double-gap exclusive diffractive Higgs boson production (1). Two gluons are exchanged between the protons. The gluon-Higgs coupling is indicated as a local vertex. The upper and lower blobs denote the gluon-proton scattering amplitude, which can be calculated in terms of the gluon GPD in the proton.

We want to identify the dominant region of integration in the loop integral. First, analogy with inclusive production of heavy particles at central rapidities suggests that the momentum fractions of the gluons producing the Higgs boson (with respect to their parent protons) are practically the same as given by the naive parton model estimate, in which one neglects the transverse momenta and virtualities of the annihilating gluons,

$$x_{1,2} \sim \frac{m_H}{\sqrt{s}} e^{\pm y}. \quad (43)$$

That is, the momentum fractions of the annihilating gluons are equal to the protons' fractional longitudinal momentum loss, $x_{1,2} \approx \xi_{1,2}$. Second, in the case of double-gap diffractive production the Sudakov formfactor associated with the Higgs boson vertex, which accounts for the absence of gluon bremsstrahlung, restricts the (spacelike) virtualities of the annihilating gluons and their transverse momenta to values of the order of some “intermediate” hard scale,

$$-k_{1,2}^2, -k_\perp^2 \sim Q_{\text{int}}^2, \quad (44)$$

with

$$m_H^2/4 \gg Q_{\text{int}}^2 \gg \Lambda_{\text{QCD}}^2. \quad (45)$$

This was demonstrated explicitly in Ref. [35], where the distribution of transverse momenta in the loop integral was studied in a model which included the LO Sudakov formfactor associated with the ggH vertex; see also Ref. [36] [64]. Expressing now the virtualities of the annihilating gluons, $k_{1,2}^2$, in terms of the decompositions (38) and (39), neglecting the proton transverse momenta relative to k_\perp , we find that Eq. (44) implies

$$x'_{1,2} = \frac{k_{2,1}^2 - k_\perp^2}{x_{2,1}s} \sim \frac{Q_{\text{int}}^2}{x_{2,1}s} \sim \frac{Q_{\text{int}}^2}{m_H \sqrt{s}} \ll x_{1,2}, \quad (46)$$

i.e., the energy and longitudinal momentum fraction of the screening gluon are substantially smaller than those of the annihilating gluons. The screening gluon does not “belong to” any of the two protons; its momentum is predominantly transverse, and it has spacelike virtuality,

$$-k^2 \approx -k_\perp^2 \sim Q_{\text{int}}^2. \quad (47)$$

In the annihilating gluons, on the other hand, longitudinal and transverse momenta contribute in equal amounts to the virtuality,

$$-k_{1,2}^2 \approx x_{1,2}x'_{2,1}s - k_\perp^2 \sim Q_{\text{int}}^2. \quad (48)$$

To summarize, the hard scattering process takes the form of the exchange of two gluons with comparable virtualities $\sim Q_{\text{int}}^2$, and transverse momenta $\sim Q_{\text{int}}$, between the protons. Of the two gluons, one carries substantial longitudinal momentum fraction of the proton, $\sim m_H/\sqrt{s}$, and annihilates with the corresponding other to make the Higgs, the other gluon represents a “Coulomb-like” exchange with small momentum fraction $\sim Q_{\text{int}}^2/(m_H\sqrt{s})$.

The important point about the two-gluon exchange process is the appearance of the intermediate hard scale, Q_{int}^2 , governing the virtualities and transverse momenta of the exchanged gluons. This allows us to make a crucial simplification in the description of the gluon–proton scattering amplitudes, which we have not yet specified so far. Namely, we argue that, in a partonic description of the proton, the gluon–proton scattering amplitude is dominated by the two gluons coupling to the same parton [37]. This approximation is analogous to the assumption of dominance of the “handbag graph” in virtual Compton scattering at large photon virtuality, Q^2 , which is well established and forms the basis of QCD factorization for this process [38, 39, 40, 41, 42]. In this approximation, the gluon–proton scattering amplitude, which is predominantly imaginary at high energies, can be calculated in terms of the generalized parton distributions (GPDs) — here, predominantly, gluon distributions — in the protons.

We do not attempt to calculate the absolute normalization of the amplitude for double-gap hard diffractive production through two-gluon exchange in terms of the GPDs; doing so would require a substantially more accurate evaluation of the two-gluon exchange graph than the qualitative estimates presented above. Fortunately, for the theory of RGS, the only information we require (in addition to the qualitative properties of the hard process derived above) is the dependence of the double-gap hard diffractive amplitude on the transverse momentum transfers to the protons, $p_{1\perp}$ and $p_{2\perp}$. For sufficiently large scales Q_{int}^2 , this dependence is described by the GPDs, even if the gluon momentum fractions in the hard amplitude and the virtuality of the exchanges are subject to integration over a certain range, and determined only in order-of-magnitude. Thus, we can state that the $p_{1\perp}$ – and $p_{2\perp}$ dependence of the double-gap hard diffractive

amplitude is proportional to

$$T_{\text{hard}} \propto H_g(x_1, \xi_1, t_1; Q^2) H_g(x_2, \xi_2, t_2; Q^2), \quad (49)$$

where

$$t_1 = p_{1\perp}^2 < 0, \quad t_2 = p_{2\perp}^2 < 0 \quad (50)$$

are the invariant momentum transfers to the proton. Here the longitudinal momentum transfers, $\xi_{1,2}$, are kinematically fixed by Eq. (37), while parton momentum fractions, $x_{1,2}$, are determined by Eq. (43) with accuracy given by Eq. (46). The resolution scale, Q^2 , at which the GPD needs to be taken here, is parametrically of the order Q_{int}^2 [*cf.* Eq. (45)], but numerically substantially larger,

$$Q^2 \sim \text{several times } Q_{\text{int}}^2. \quad (51)$$

This follows from the fact that, by convention, Q^2 determines the upper limit of the transverse momenta in the parton distribution, while Q_{int}^2 is a measure of the dominant (average) values in the distribution, which for a $1/k_\perp^2$ distribution is significantly lower than the upper limit.

To conclude this discussion, some comments concerning QCD evolution and the modeling of the GPDs are in order. First, in Higgs boson production at the LHC we are dealing with the gluon GDP at $x, \xi \sim 10^{-2}$ and $x' \ll x$, where it can legitimately be calculated by applying QCD evolution to a diagonal GPD at a lower scale (*cf.* the discussion in Section III). Second, at LHC energies the typical momentum fraction of the screening gluon reaches values $x'_{1,2} \sim 10^{-6}$ for $Q^2 \sim \text{few GeV}^2$, *cf.* Eq. (46). For such low values of x the use of DGLAP evolution in principle requires justification. However, as explained in detail in Ref. [9], for such values of x the kinematic conditions still restrict the actual number of radiated gluons to a few, so that NLO DGLAP and resummed BFKL evolution give similar results, see Ref. [43] for a review. In this sense, the use of GPDs generated by DGLAP evolution seems to be appropriate. Third, one may wonder about the breakdown of the pQCD calculation of the hard reaction amplitude due to the growth of the gluon density at small x within the DGLAP approximation — the BDL, see Ref. [9] and references therein. This should not be a problem in the present context, since the BDL affects only collisions at central impact parameters, where the diffractive amplitude is anyway suppressed due to the vanishing rapidity gap survival probability (see Sec. V below).

B. Combining hard and soft interactions

In the second step, we formalize the interplay of hard and soft interactions in the amplitude of the hadronic diffractive process, Eq. (1). To this end, we invoke the parton picture of the proton wavefunction, as developed

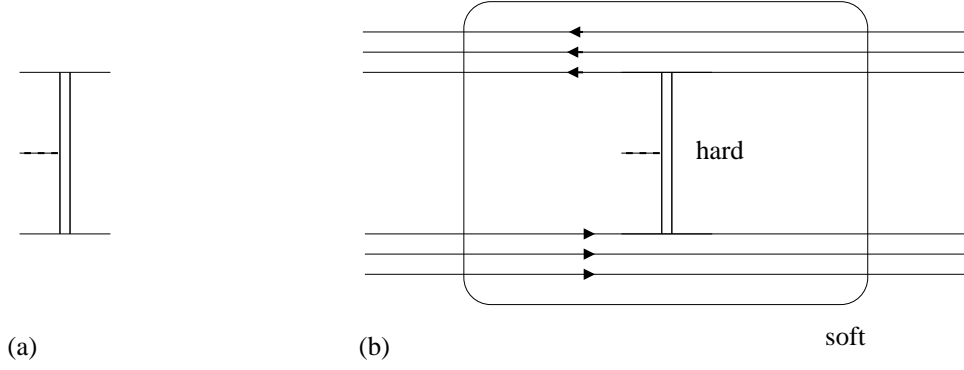


FIG. 5: Schematic illustration of hard and soft interactions in the parton picture of double-gap exclusive diffractive pp scattering. (a) The hard scattering process producing the large-mass system (Higgs, dijet) is represented by a local operator in parton degrees of freedom. (b) Hard and soft interactions are approximately independent since they happen over widely different time- and distance scales.

by Gribov [8]. We consider the process (1) in the CM frame, in which the two protons in the initial state have longitudinal momenta $\pm\sqrt{s}/2$, and zero transverse momentum, $\mathbf{p}_{1\perp}, \mathbf{p}_{2\perp} = 0$. Since $m_H \ll \sqrt{s}/2$, angular momentum conservation implies that the reaction amplitude is approximately diagonal in the transverse coordinates of the colliding protons (*i.e.*, in impact parameter) as in two-body elastic scattering at high energies. We thus consider partonic configurations centered around the transverse centers of the two protons, in which the partons carry fractions of the longitudinal momentum of the respective proton. We may regard the hard scattering process as an operator in the basis of these partonic states, denoted by \hat{V}_{hard} . Soft interactions, which build up the partonic wavefunctions, are governed by a soft Hamiltonian, \hat{H}_{soft} . While we do not know their explicit form, we can nevertheless state some important properties of these operators:

1. \hat{V}_{hard} is local in time (instantaneous) on the typical timescale of soft interactions,
2. \hat{V}_{hard} is local in transverse position on the distance scale over which the transverse spatial distribution of partons in the protons changes due to soft interactions,
3. \hat{V}_{hard} preserves the number of partons, since scattering of both gluons from the same parton dominates in the hard regime.
4. \hat{V}_{hard} preserves the helicity of the colliding partons, because in a perturbative gauge theory the dominant contribution to the interaction of partons over large rapidity intervals comes from the parton helicity-conserving component of the propagator of the exchanged gluon [44].

As a consequence of these properties, we conclude that the operator of the hard reaction commutes with the

Hamiltonian of soft interactions,

$$[\hat{V}_{\text{hard}}, \hat{H}_{\text{soft}}] = 0. \quad (52)$$

This is the mathematical statement of the independence of hard and soft interactions in diffraction. A schematic illustration of this picture is given in Fig. 5. We shall refer to Eq. (52) and the formulas derived from it as the independent interaction approximation.

The amplitude for the double-gap exclusive diffractive process (1) is then determined by the matrix element

$$T_{\text{diff}} = \langle p'_1 p'_2 | \hat{S}_{\text{soft}}(\infty, 0) \hat{V}_{\text{hard}} \hat{S}_{\text{soft}}(0, -\infty) | p_1 p_2 \rangle, \quad (53)$$

where

$$\hat{S}_{\text{soft}}(t_2, t_1) \equiv T \int_{t_1}^{t_2} dt \exp(it\hat{H}_{\text{soft}}) \quad (54)$$

is the time evolution operator due to soft interactions (we have put the time of the hard interaction at $t = 0$). Because of Eq. (52), the operator \hat{V}_{hard} commutes with the soft time evolution operator. Using the property

$$\hat{S}_{\text{soft}}(\infty, 0) \hat{S}_{\text{soft}}(0, -\infty) = \hat{S}_{\text{soft}}(\infty, -\infty) \equiv \hat{S}_{\text{soft}}, \quad (55)$$

where \hat{S}_{soft} is the S -matrix due to soft interactions, we obtain

$$T_{\text{diff}} = \langle p'_1 p'_2 | \hat{V}_{\text{hard}} \hat{S}_{\text{soft}} | p_1 p_2 \rangle. \quad (56)$$

Thus, the amplitude is expressed in terms of the observable matrix elements of the soft S -matrix, and the operator \hat{V}_{hard} , calculable in QCD at the partonic level. Eq. (56) is the fundamental expression for discussing the physics of RGS within our approach.

C. Suppression of inelastic diffraction

In the next step, we evaluate the amplitude for the double-gap exclusive diffractive process based on

Eq. (56), by inserting “intermediate” states (actually, states at $t = \infty$) between the operators. In principle, one needs to sum over all diffractive states (elastic and inelastic) produced by the operator \hat{V}_{hard} . An important question is which states can give large contributions to the matrix element. In fact, it turns out that the different preferences of hard and soft interactions severely restrict the range of states which can effectively contribute.

Simple arguments show that large-mass diffractive states should make a negligible contribution to Eq. (56). If the two hard gluons in the hard interaction are attached to two different partons in the proton, the inelastic states predominantly produced are two jets and gluon bremsstrahlung. It is virtually impossible to produce such states in soft interactions, hence they cannot contribute to Eq. (56). If the two hard gluons are attached to the same parton, the cross section of inelastic diffraction is small for small t because of the small overlap integral with the inelastic state (most of the overlap is with the elastic state), while for large t one produces a single parton with transverse momentum $p_{\perp} \sim \sqrt{-t}$, which again is a state difficult to reach through soft interactions. In addition, for $t \neq 0$ soft diffraction at LHC energies is known to be dominated by the spin-flip amplitude, which further suppresses the overlap integral. Together, this restricts the possible mass range of diffractively produced states to $M_{\text{diff}}^2 \sim \text{few GeV}^2$.

For a more quantitative estimate, we suppose that the state produced through inelastic diffraction has the form $|pp\rangle + \epsilon|pX\rangle$, where the state X is different from the proton, and ϵ is a small correction. We can then estimate ϵ from the Schwarz inequality:

$$\frac{\epsilon}{2} = \sqrt{\frac{\sigma_{\text{soft}}(pp \rightarrow Xp) \sigma_{\text{hard}}(pp \rightarrow Xp)}{\sigma_{\text{soft}}(pp \rightarrow pp) \sigma_{\text{hard}}(pp \rightarrow pp)}}, \quad (57)$$

where $\sigma_{\text{hard}}(pp \rightarrow pX)$ is the cross section for the production of the state $|pX\rangle$ by the operator \hat{V}_{hard} . Analysis of the Tevatron data (for a review, see Ref. [45]) shows that the fraction of diffractive events in soft collisions decreases with increasing energy, and that the distribution over the excitation mass is $\propto 1/M_X^2$. As a result, we expect that at the LHC energy $\epsilon \leq 2 \cdot 10^{-2}$. Thus, the diffractively produced state is actually the $|pp\rangle$ state, and the contributions from inelastic diffraction are small.

The small overlap between hard and soft diffraction can also be understood as the result of the different impact parameter dependence of both types of processes. Hard diffraction occurs mostly at small impact parameters, $b^2 \sim B_g$. Soft diffraction, because of the approach to the BDL, occurs mostly at large impact parameters, $b^2 \sim B$, which, moreover, rapidly grow with the collision energy. We note again that the peripheral nature of soft diffraction was established already within Reggeon field theory, where it was found that the BDL solves the consistency problem associated with the triple Reggeon formula [20].

The restriction to the pp intermediate state turns

Eq. (56) into a tool for quantitative evaluation of the diffractive amplitude and the RGS. In particular, with the pp intermediate state we can approximate the matrix element of the soft-interaction time evolution operator by that of the full S -matrix, *i.e.*, the pp elastic scattering amplitude, which is known experimentally; see Section II. For this approximation to be legitimate it is crucial that scattering at small impact parameters turns out to be strongly suppressed due to the approach to the BDL in pp elastic scattering, as will be seen from the results of Section V. The diffractive process is thus dominated by large impact parameters, where pp elastic scattering is dominated by soft interactions.

In the studies of double-gap exclusive diffraction based on the pomeron model of Ref. [4], inelastic intermediate states were effectively included by way of a two-component formalism (however, no explicit non-diagonal “transition” GPDs were introduced). We have argued here that these contributions are strongly suppressed, because of the small overlap of states accessible in hard and soft interactions. We shall comment on the implications of this for the numerical values of the RGS probability in Section V B

D. Evaluation of the diffractive amplitude

It remains to actually evaluate the matrix element (56) with $|pp\rangle$ intermediate states, using the specific form of the hard scattering amplitude and the pp elastic scattering amplitude. We insert a set of pp intermediate states in the form

$$\int \frac{d^3 p_1''}{(2\pi)^3 \sqrt{s}} \int \frac{d^3 p_2''}{(2\pi)^3 \sqrt{s}} |p_1'' p_2''\rangle \langle p_1'' p_2''|, \quad (58)$$

where we have approximated the energy of the individual protons by $\sqrt{s}/2$. The matrix element of the operator \hat{V}_{hard} between the two-proton states is, by definition, given by [cf. Eqs. (49)]

$$\begin{aligned} \langle p_1' p_2' | \hat{V}_{\text{hard}} | p_1'' p_2'' \rangle &= \kappa(s, \xi_1, \xi_2) \\ &\times F_g(x_1, \xi_1, \tilde{t}_1; Q^2) \\ &\times F_g(x_2, \xi_2, \tilde{t}_2; Q^2), \end{aligned} \quad (59)$$

where

$$\tilde{t}_1 \equiv -(\mathbf{p}_{1\perp}' - \mathbf{p}_{1\perp}'')^2, \quad (60)$$

$$\tilde{t}_2 \equiv -(\mathbf{p}_{2\perp}' - \mathbf{p}_{2\perp}'')^2. \quad (61)$$

The factor

$$\begin{aligned} \kappa(s, \xi_1, \xi_2) &\equiv C_{\text{hard}} \\ &\times H_g(x_1, \xi_1, t_1 = 0) \\ &\times H_g(x_2, \xi_2, t_2 = 0) \end{aligned} \quad (62)$$

represents the symbolic result for the absolute normalization of amplitude of the hard scattering process; it contains the amplitude of the two-gluon exchange process,

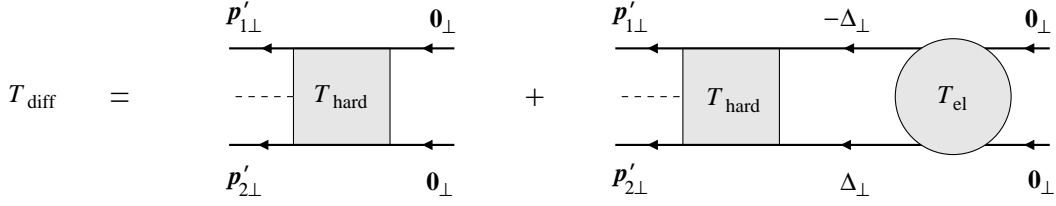


FIG. 6: The amplitude for double-gap exclusive hard diffraction in momentum representation, Eqs. (66)–(69). The first term is the amplitude of the hard reaction alone, the second term the correction due to soft elastic rescattering. Only the transverse momenta of the protons are indicated; the momentum transfer due to soft elastic scattering is Δ_\perp .

C_{hard} , including the information about the ggH coupling given by the electroweak theory, as well as the information about the gluon GPD in the colliding protons at $t = 0$. The information about the transverse momentum dependence of the amplitude is contained in the two-gluon formfactors, F_g , cf. Eq.(19). Furthermore, we replace in Eq. (56)

$$\hat{S}_{\text{soft}} \rightarrow \hat{S} = 1 + (\hat{S} - 1), \quad (63)$$

and use the fact that the matrix element of the operator $\hat{S} - 1$ is given by

$$\begin{aligned} \langle p_1'' p_2'' | \hat{S} - 1 | p_1 p_2 \rangle &= i(2\pi)^4 \delta^{(4)}(p_1'' + p_2'' - p_1 - p_2) \\ &\times (4\pi) T_{\text{el}}(s, t), \end{aligned} \quad (64)$$

with

$$t = -(\mathbf{p}_{1\perp}'' - \mathbf{p}_{1\perp})^2 = -(\mathbf{p}_{2\perp}'' - \mathbf{p}_{2\perp})^2. \quad (65)$$

Finally, taking into account that at high energies the energy-conserving delta function in Eq. (64) effectively conserves longitudinal momentum, and combining the contributions from the two terms in Eq. (63), we obtain

$$\begin{aligned} T_{\text{diff}}(\mathbf{p}'_{1\perp}, \mathbf{p}'_{2\perp}) &= \int \frac{d^2 \Delta_\perp}{(2\pi)^2} \\ &\times \kappa F_g(x_1, \xi_1, \tilde{t}_1; Q^2) F_g(x_2, \xi_2, \tilde{t}_2; Q^2) \\ &\times \left[(2\pi)^2 \delta^{(2)}(\Delta_\perp) + \frac{4\pi i}{s} T_{\text{el}}(s, t) \right], \end{aligned} \quad (66)$$

where now

$$\tilde{t}_1 \equiv -(\mathbf{p}'_{1\perp} - \Delta_\perp)^2, \quad (67)$$

$$\tilde{t}_2 \equiv -(\mathbf{p}'_{2\perp} + \Delta_\perp)^2, \quad (68)$$

$$t \equiv -\Delta_\perp^2. \quad (69)$$

This result has a simple interpretation (see Fig. 6). The first term in the brackets represents the amplitude of the hard reaction alone. The second term represents the contribution in which the hard reaction is accompanied by soft elastic rescattering with transverse momentum transfer Δ_\perp . The total amplitude is the coherent superposition of the two contributions. We note that the form of this result is analogous to the well-known absorption corrections in Regge phenomenology, in which

an elementary Regge pole amplitude is modified by elastic rescattering.

It is instructive to convert the result (66) to the transverse coordinate representation. Substituting the Fourier representation of the gluon GPDs, Eq. (22), and the representation of the pp elastic amplitude in terms of the profile function, Eq. (2), and using standard Fourier transform manipulations, we obtain

$$\begin{aligned} T_{\text{diff}}(\mathbf{p}'_{1\perp}, \mathbf{p}'_{2\perp}) &= \int d^2 b \int d\rho_1 \int d\rho_2 \\ &\times \delta^{(2)}(\mathbf{b} - \boldsymbol{\rho}_1 + \boldsymbol{\rho}_2) e^{-i(\mathbf{p}'_{1\perp} \boldsymbol{\rho}_1) - i(\mathbf{p}'_{2\perp} \boldsymbol{\rho}_2)} \\ &\times \kappa F_g(x_1, \xi_1, \boldsymbol{\rho}_1; Q^2) F_g(x_2, \xi_2, \boldsymbol{\rho}_2; Q^2) \\ &\times [1 - \Gamma(s, \mathbf{b})]. \end{aligned} \quad (70)$$

Here the scattering amplitude is represented as the coherent superposition of amplitudes corresponding to pp scattering at given transverse displacement (impact parameter), \mathbf{b} . The amplitude for the hard process is proportional to the product of the transverse spatial gluon transition densities at positions $\boldsymbol{\rho}_{1,2}$ relative to the centers of the respective protons, with the three transverse vectors satisfying the triangular condition $\boldsymbol{\rho}_1 - \boldsymbol{\rho}_2 = \mathbf{b}$ (see Fig. 7). The modifications due to elastic rescattering now take the form of a multiplication of the hard scattering amplitude with the “absorption factor,” $1 - \Gamma(s, \mathbf{b})$. Note that the modulus squared of this factor can be interpreted as the probability for “no inelastic interaction” in pp scattering at a given impact parameter, cf. Eq. (4). This interpretation will be explored further in Sec. V.

Our partonic approach allows us to calculate the amplitude for double-gap exclusive diffraction in a model-independent way in terms of the gluon GPD and the phenomenological pp elastic scattering amplitude; see Eqs. (66–70). In Ref. [5] such processes were studied using a model of elastic pp scattering which included the enhanced eikonal series of single Pomeron exchanges and the triple-Pomeron vertex to describe the soft spectator interactions. The expression for the amplitude in the case of a single Pomeron exchange in that model (and without inelastic intermediate states) would formally coincide with our expressions (66–70). Whether the same is true for the full amplitude in that model is less clear; cf. the discussion of the numerical results in Section V B below.

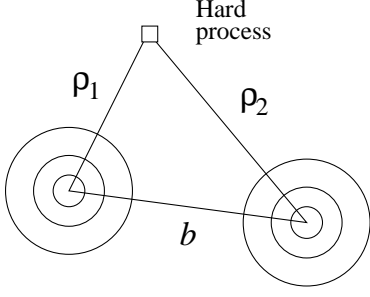


FIG. 7: Illustration of the transverse coordinate representation of the diffractive amplitude, Eq. (70). The hard scattering process is local in transverse space. The centers of the colliding protons are displaced by the distance $b = |\mathbf{b}|$, and $\rho_{1,2} = |\rho_{1,2}|$ are the distances from the centers to the point of the hard process.

V. THE RAPIDITY GAP SURVIVAL PROBABILITY

We now use our general result for the amplitude of double-gap exclusive diffractive processes in the independent interaction approximation, Eq. (70), to calculate the RGS probability for such processes. At this level of approximation, we shall recover a simple “geometric” expression for the RGS probability, which permits a probabilistic interpretation and was heuristically derived in Refs. [9, 10, 11]. We discuss the impact parameter dependence of RGS and stress the crucial role of the BDL in stabilizing the numerical estimates ensuring a model-independent result.

A. Impact parameter representation

In order to compute the cross section for double-gap exclusive diffractive production of a given state at fixed rapidity, we integrate the modulus squared of the amplitude (70) over the final proton transverse momenta. By standard Fourier transform manipulations we obtain

$$\sigma_{\text{diff}} = (\text{kinematic factors}) \times \int \frac{d^2 p'_{1\perp}}{(2\pi)^2} \int \frac{d^2 p'_{2\perp}}{(2\pi)^2} \times |T_{\text{diff}}(\mathbf{p}'_{1\perp}, \mathbf{p}'_{2\perp})|^2 \quad (71)$$

$$= (\text{const}) \times \int d^2 \rho_1 \int d^2 \rho_2 F_g^2(\rho_1) F_g^2(\rho_2) \times |1 - \Gamma(\rho_2 - \rho_1)|^2 \quad (72)$$

(for brevity we suppress all arguments except the transverse coordinates in F_g and Γ). The RGS probability due to soft interactions [7], by definition, is given by the ratio of the cross section of the physical double-gap diffractive process (72) to the cross section of the hypothetical process with the same hard scattering subprocess but with no soft spectator interactions, corresponding to expres-

sion (72) with $\Gamma \equiv 0$,

$$S^2 \equiv \frac{\sigma_{\text{diff}}(\text{physical})}{\sigma_{\text{diff}}(\text{no soft interactions})}. \quad (73)$$

We can cast this ratio in a simple form. We rewrite the convolution integral in Eq. (72) by inserting unity in the form (*cf.* Fig. 7)

$$\int d^2 b \delta^{(2)}(\mathbf{b} + \rho_1 - \rho_2), \quad (74)$$

and introduce a normalized impact parameter distribution,

$$P_{\text{hard}}(\mathbf{b}) \equiv \int d^2 \rho_1 \int d^2 \rho_2 \delta^{(2)}(\mathbf{b} + \rho_1 - \rho_2) \times \frac{F_g^2(\rho_1)}{\left[\int d^2 \rho'_1 F_g^2(\rho'_1) \right]} \frac{F_g^2(\rho_2)}{\left[\int d^2 \rho'_2 F_g^2(\rho'_2) \right]}, \quad (75)$$

which satisfies

$$\int d^2 b P_{\text{hard}}(\mathbf{b}) = 1. \quad (76)$$

In terms of this distribution the RGS probability (73) is expressed as

$$S^2 = \int d^2 b P_{\text{hard}}(\mathbf{b}) |1 - \Gamma(\mathbf{b})|^2. \quad (77)$$

This result agrees with the expression for the RGS probability derived heuristically in Refs. [9, 10, 11] [65]. For the comparison of our result for the RGS probability with that obtained with the pomeron model of Ref. [5] we refer to Section VB below; see also the comments at the end of Sec. IV D.

Expression (77) for the RGS probability allows for a simple probabilistic interpretation. Consider a pp collision at given impact parameter, $b = |\mathbf{b}|$. Since the hard two-gluon exchange process is effectively local in transverse space, the probability for it to happen is proportional to the product of the squared transverse spatial distributions of gluons in the two colliding protons, integrated over the transverse plane, as given by the numerator of Eq. (75). Consider now a hypothetical sample of pp events with the two-gluon induced hard scattering process, but an otherwise arbitrary (non-diffractive) final state. By the laws of probability, the distribution of impact parameters in this sample is given by the normalized distribution $P_{\text{hard}}(\mathbf{b})$, Eq. (75). A diffractive event results if the spectator systems of the two protons do not interact inelastically. The probability for this to happen in a pp collision at fixed b is given by $|1 - \Gamma(\mathbf{b})|^2$, *cf.* Eq. (4), in analogy to the well-known formula for inelastic scattering in non-relativistic theory [46]. The RGS probability, which is defined as the fraction of diffractive events in the sample of all events containing the same hard scattering process, is then given by the average of

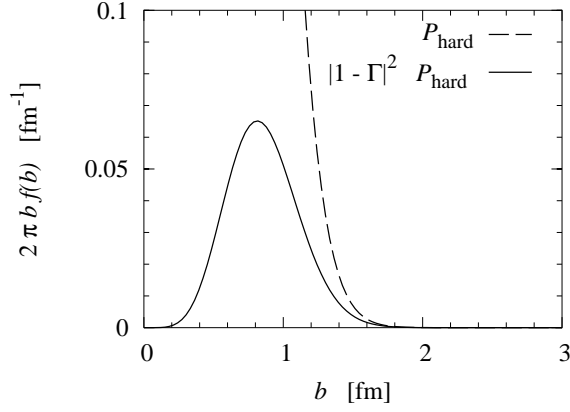


FIG. 8: The integrand (impact parameter distribution) in the RGS probability, Eq. (77), for Higgs boson production at the LHC energy. Dashed line: b -distribution of the hard two-gluon exchange, $P_{\text{hard}}(b)$, Eq. (75), evaluated with the exponential parametrization of the two-gluon form-factor, Eq. (33) with $B_g = 3.24 \text{ GeV}^{-2}$. Solid line: The product $P_{\text{hard}}(b)|1 - \Gamma(b)|^2$, evaluated with the exponential parametrization, Eq. (12), with $B = 21.8 \text{ GeV}^{-2}$. The vanishing of $|1 - \Gamma(b)|^2$, at small b , *cf.* Fig. 1, strongly suppresses contributions from small impact parameters. Note that the plot shows $2\pi b$ times the functions of impact parameter; the small- b part of the dashed curve [distribution $P_{\text{hard}}(b)$] would be close to the left boundary of the plot and was omitted for better legibility. The RGS probability, S^2 , is given by the area under the solid curve.

this function with the normalized b -distribution in the sample, Eq. (77).

It needs to be stressed that the impact parameter of a single pp event is not observable, being a microscopic quantity beyond the reach of any experimental apparatus. In the above arguments, the impact parameter plays the role of a randomly chosen external parameter. However, using information about the transverse spatial distribution of gluons in the proton from independent measurements, we can calculate the probability for certain hard processes in a pp collision as a function of the impact parameter, and thus infer the distribution of impact parameters in a sample of events with the same hard process. This logic was used in Ref. [18] to devise a trigger on central collisions in inclusive pp scattering by requiring hard dijet production at small rapidities. Here we use the same strategy to model soft spectator interactions in double-gap exclusive diffractive pp scattering.

The integrand in Eq. (77) describes the effective distribution of impact parameters in a sample of double-gap diffractive events, and reflects the interplay of hard and soft interactions at the cross section level. The probability for the hard process, $P_{\text{hard}}(\mathbf{b})$, favors small impact parameters, which maximize the overlap of the large- x gluon distributions in the protons, and vanishes for $b^2 \gg 1/B_g$. The probability for no inelastic soft interactions, $|1 - \Gamma(\mathbf{b})|^2$, favors large impact parameters, which increase the chances for the protons to stay intact, and

vanishes for $b^2 \ll 1/B$ where pp scattering approaches the BDL. The product of the two probabilities is suppressed both at small and at large b , and thus concentrated at intermediate values of b .

This point can nicely be illustrated with the Gaussian parametrizations of the transverse spatial distribution of gluons, Eq. (34), and the pp elastic profile function, Eq. (12). With the Gaussian form (34), the convolution integral in Eq. (75) can be computed analytically,

$$P_{\text{hard}}(\mathbf{b}) = \frac{\exp[-\mathbf{b}^2/(2B_g)]}{2\pi B_g}. \quad (78)$$

This function is shown by the dashed line in Fig. 8. The integrand of Eq. (77) is given by

$$P_{\text{hard}}(\mathbf{b}) |1 - \Gamma(\mathbf{b})|^2 = \frac{1}{2\pi B_g} \exp\left(-\frac{\mathbf{b}^2}{2B_g}\right) \left[1 - \exp\left(-\frac{\mathbf{b}^2}{2B}\right)\right]^2, \quad (79)$$

and is shown by the solid line in Fig. 8. It is suppressed both for $b^2 \ll 1/B$ (because of the “blackness” of the pp amplitude) and for $b^2 \gg 1/B_g$ (because of the vanishing of the overlap of the two gluon distributions), and thus concentrated at intermediate values of b . The maximum of $2\pi b$ times the combined distribution is at

$$b^2 \approx 5B_g \quad (B_g \ll B). \quad (80)$$

We see that within our two-scale picture of the transverse structure of hard and soft interactions, *cf.* Fig. 2, the dominant impact parameters in double-gap exclusive diffractive processes are determined by B_g — the smaller of the two areas —, but may be numerically large because of a large numerical factor. The RGS probability, Eq. (77), is given by the integral of $2\pi b$ times Eq. (79) (*i.e.*, the area under the solid curve in Fig. 8), and can be computed analytically,

$$S^2 = \frac{2B_g^2}{(B + B_g)(B + 2B_g)} \approx \frac{2B_g^2}{B^2} \quad (B_g \ll B). \quad (81)$$

The gap survival probability is of the order $(B_g/B)^2$, *i.e.*, it is proportional to the square of the ratio of the transverse area occupied by hard gluons to the area corresponding to soft interactions. Thus, our two-scale picture offers a parametric argument for the smallness of the rapidity gap survival probability.

The approach to the black-disk limit in pp scattering at high energies, *i.e.*, the fact that $\Gamma(\mathbf{b}) \rightarrow 1$ at small b , plays a crucial role in determining the numerical value of the RGS probability and ensuring stability of our calculation with respect to variation of the parameters. A small deviation of the profile function from unity at $b = 0$, of the form $\Gamma(\mathbf{b} = 0) = 1 - \epsilon$ with $\epsilon \ll 1$, would change the result for the gap survival probability to

$$S^2 \rightarrow S^2|_{\text{BDL}} + \epsilon^2 \quad (82)$$

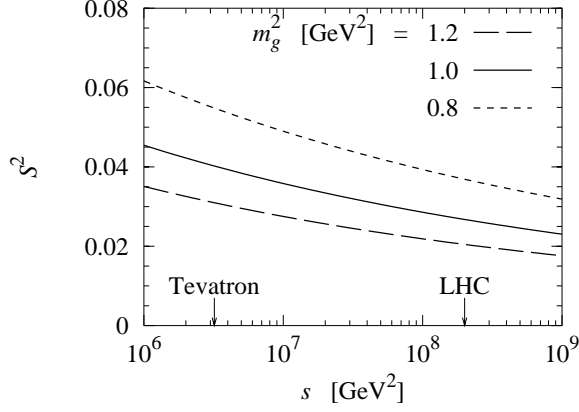


FIG. 9: The RGS probability for double-gap exclusive diffractive processes, Eq. (77), as a function of the squared CM energy, s . The Tevatron and LHC energies are marked by arrows. Shown are the results obtained with the dipole parametrization of the two-gluon formfactor (31), for different values of the mass parameter, m_g^2 . The value $m_g^2 = 1 \text{ GeV}^2$ is appropriate for Higgs boson production at the LHC at central rapidities. The profile function of the pp elastic amplitude was taken from Ref. [17] (*cf.* Fig. 1).

[here we have used that $B_g \ll B$, and that the integral of P_{hard} is unity, *cf.* Eq. (76)]. The approach to the BDL effectively eliminates $\Gamma(\mathbf{b} = 0)$ as a parameter in our calculation. We stress again that the experimental data as well as theoretical arguments indicate that the BDL is indeed reached in pp scattering at small impact parameters at the LHC energy.

B. Numerical estimates

For a numerical estimate of the gap survival probability we evaluate Eq. (77) with the dipole parametrization of the two-gluon formfactor, Eq. (31), and the parametrization of the pp elastic amplitude of Ref. [17]. For Higgs production at the LHC ($\sqrt{s} = 14 \text{ TeV}$) at central rapidities the momentum fractions of the annihilating gluons are $x_{1,2} \sim 10^{-2}$ (at a scale $Q^2 \ll m_H^2$). For such values of x in principle the contributions of the nucleon's pion cloud to the gluon density at transverse distances $\rho \sim 1/(2M_\pi)$ need to be taken into account; see Section III. As we shall explain below, these contributions to the gluon density involve correlations in the nucleon wavefunction, which effectively reduce their contribution to RGS, and should not be included in the estimate based on Eq. (77). We therefore use in our estimate at the LHC energy the simple dipole formfactor with $m_g^2 \approx 1 \text{ GeV}^2$, which does not include the pion cloud contribution. With this choice of parameters Eq. (77) gives for the RGS probability for Higgs production at the LHC

$$S^2 = 0.027. \quad (83)$$

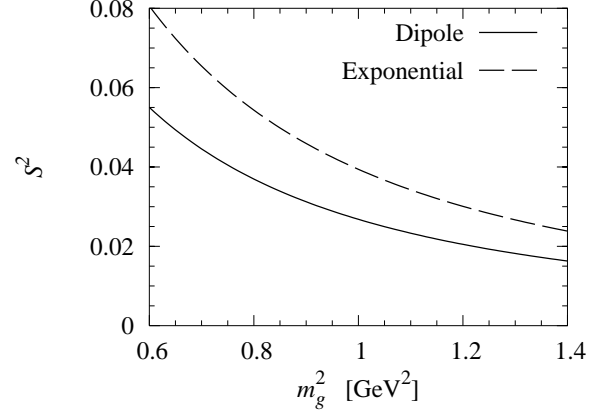


FIG. 10: Dependence of the RGS probability for double-gap exclusive diffractive Higgs production at the LHC, Eq. (77), on the mass parameter in the dipole parametrization of the two-gluon formfactor, m_g^2 , Eq. (31). Also shown are the results obtained with the exponential parameterization, Eq. (33), with $B_g = 3.24/m_g^2$, *cf.* Eq. (35) and Fig. 3. The profile function of the pp elastic amplitude in both cases is the one of Ref. [17].

The energy dependence of the RGS probability is shown in Fig. 9, for various values of the mass parameter of the two-gluon formfactor, m_g^2 . At the Tevatron energy ($\sqrt{s} = 1.9 \text{ TeV}$), the gluon momentum fractions $x_{1,2}$ are of the order $\sim 10^{-1}$, for which the pion cloud contributions to the gluon density are naturally absent. While a mass parameter $m_g^2 = 1 \text{ GeV}^2$ is still reasonable in this situation, even higher values m_g^2 might be relevant in this case. Taking into account this effective change of m_g^2 with s via the $x_{1,2}$ -dependence, the actual variation of the RGS probability between the LHC and the Tevatron energies is less pronounced than it appears from the fixed- m_g^2 curves in Fig. 9.

Figure 10 (solid line) shows the dependence of the RGS probability at the LHC energy on the mass parameter in the dipole parametrization of the two-gluon formfactor, m_g^2 , Eq. (31). The value of S^2 strongly increases with decreasing m_g^2 , *i.e.*, with increasing radius of the transverse spatial distribution of gluons, similar to the behavior found with the simple exponential parametrizations, Eq. (81). To illustrate the sensitivity of our numerical predictions to the shape of the two-gluon formfactor, we also show the results for S^2 obtained when replacing the dipole formfactor by the exponential, Eq. (33), with $B_g = 3.24/m_g^2$, *cf.* Eq. (35). (Figure 10, dashed line). One sees that the numerical values are rather different, in spite of the apparent similarity of the two formfactors over a wide range, $|t| \lesssim 1 \text{ GeV}^2$ (*cf.* Fig. 3). Comparing the two curves of Figure 10, we estimate the uncertainty of our numerical prediction for the RGS probability due to the uncertainty of the shape of the two-gluon formfactor to be at least $\sim 30\%$.

In a similar way, we can estimate the uncertainty of

the RGS probability due to the uncertainty of the profile of the pp elastic amplitude. Comparing the numerical values obtained from Eq. (77) with the parametrization of Ref. [17] and with the simple exponential parametrization, Eqs. (11) and (12), for the same two-gluon formfactor, we again find variations of the order of $\sim 30\%$.

The relatively high sensitivity of the numerical estimates to the shape of the two-gluon formfactor and the profile function of the pp elastic amplitude can be understood as a result of the peculiar interplay of hard and soft interactions in Eq. (77). The different impact parameter dependence of hard and soft interactions (*cf.* Fig. 8 and the discussion above) essentially eliminates contributions from the regions corresponding to the “bulk” of the individual distributions, $P_{\text{hard}}(\mathbf{b})$ and $|1 - \Gamma(\mathbf{b})|$, allowing for significant strength only in an intermediate region of impact parameters, where there is considerable sensitivity to the shape of the distributions. This seems to be a principal feature of estimates of the RGS probability based on Eq. (77).

Detailed numerical studies of the RGS probability were made within the eikonalized Pomeron model for soft interactions, see Ref. [4] for a summary. We would like to comment on these estimates from the perspective of our approach. As we already noted, the approach of Ref. [4] includes contributions from inelastic intermediate states (albeit without introducing non-diagonal “transition” GPDs). We have argued that within the independent interaction approximation these contributions are strongly suppressed and should not be included, see Section IV C. Nevertheless, the numerical result for the RGS probability in Higgs boson production in double-gap diffraction at the LHC quoted in Ref. [5], $S^2 = 0.023$ [66], is rather similar to our estimate (83). Note that Ref. [5] ascribes an uncertainty of $\sim 50\%$ to this value; we have estimated a similar uncertainty for our result due to the combined uncertainties in the profile function and the two-gluon formfactor (see above). It is interesting to ask why the results are so similar when the two approaches differ in their treatment of inelastic diffraction. In order to clarify this question, we have evaluated our expression for the RGS probability, Eq. (77), with the profile function of the pp elastic amplitude obtained within the model of Ref. [4], which was kindly provided to us by M. Ryskin; we emphasize that this is not the same as evaluating the expression for the RGS probability given in Ref. [4]. Using the exponential form of the two-gluon formfactor (33) with parameters $B_g = (4, 5.5, 10.1) \text{ GeV}^{-2}$ we obtain in this way $S^2 = (0.042, 0.069, 0.157)$, which should be compared to the results quoted in Ref. [4], $S^2 = (0.02, 0.04, 0.11)$. One sees that our Eq. (77) gives systematically larger values than the approach of Ref. [4] for the same profile function and the same two-gluon formfactor. This difference should be attributed to the effect of inelastic diffraction. What is then quoted as the final estimate of S^2 depends on the preferred value of B_g . The RGS probability strongly decreases with B_g , *cf.* Eq. (81) and

Fig. 10. For Higgs production at the LHC we use a value of $B_g = 3.24 \text{ GeV}^{-2}$ (corresponding to a mass parameter in the dipole parametrization of $m_g^2 = 1 \text{ GeV}^2$), which is based on analysis of the J/ψ photoproduction data over a wide range of energies and takes into account the effects of QCD evolution (*cf.* Section III). With this value we obtain $S^2 = 0.030$ for the exponential two-gluon formfactor and the profile function of Ref. [4]. This value of B_g is lower than the range of values considered in Ref. [4] (our $B_g = 2b$ in the notation of that paper). The value of B_g for Higgs production at the LHC taken in Ref. [5] is $B_g = 4 \text{ GeV}^{-2}$, which results in $S^2 = 0.02$ in their model. One sees that the different values of B_g partly compensate the differences due to the treatment of inelastic diffraction in the two approaches. We thus conclude that the similarity of the final numerical estimate of Ref. [5] with our results is somewhat accidental. In any case, the differences between the numerical results of both approaches are within the estimated uncertainties.

Potentially more important than the uncertainties of our calculation of the RGS probability within the independent interaction approximation are effects of possible correlations between hard and soft interactions. These effects can naturally be incorporated into our partonic picture, and further decrease the RGS probability compared to the independent interaction approximation (see Section VI B).

VI. BEYOND THE INDEPENDENT INTERACTION APPROXIMATION

Our treatment of RGS so far was based on the idea that hard and soft interactions are approximately independent because they proceed over widely different time- and distant scales. It is clear that this approximation has certain limitations, concerning both the range of its applicability and its accuracy. In this Section we discuss various physical effects which violate the assumption of independence of hard and soft interactions and give rise to corrections to the estimates of the RGS probability of Section V. These are (a) the increase of hard screening corrections with energy, (b) correlations between hard and soft interactions. These corrections have not been considered in previous treatments of RGS in Refs. [5, 35, 36].

A. Hard screening corrections

The independent interaction approximation relies on the assumption of widely different characteristic scales of hard and soft processes. However, the difference between the two scales tends to decrease, and may even disappear, at high energies, because of the fast increase of the amplitudes of hard processes with energy. One example of this effect is the BDL in pp elastic scattering at central impact parameters, which can be explained both on the basis of hard and soft interactions (see Section II). In

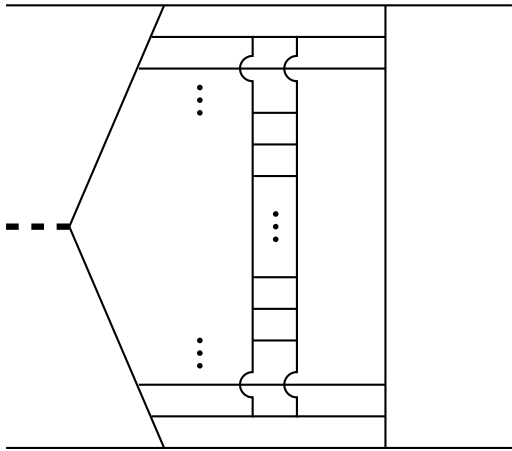


FIG. 11: A typical diagram describing hard screening corrections to the hard amplitude for double-gap diffractive production. Shown is only the generic structure of the partonic ladders; the dominant contribution comes from gluons.

diffractive scattering, the increase of hard amplitudes at high energies leads to a reduction of the RGS probability relative to the estimates presented in Section V.

One specific mechanism which can lead to qualitative changes of the hard scattering process at high energies is “local” absorption of the hard scattering amplitude for diffractive production. This corresponds to the familiar attenuation of the hard gluon exchange diagram for Higgs production, but by a two-gluon ladder (see Fig. 11). Here the two-gluon ladder is attached to the partons which emitted the gluons involved in the Higgs production. Actually, in order to regularize the infrared divergences present in the two-gluon ladder we may consider instead the amplitude for the scattering of two colorless dipoles, in which the typical virtuality of the “constituents” is k_{\perp}^2 ; a second parton with such virtuality is anyway present as a result of QCD evolution. The amplitude of the additional interaction is then suppressed relative to the original hard amplitude by a factor $\alpha_s^2(k_{\perp}^2/\tilde{k}_{\perp}^2)(x_0/x)^\lambda$, where \tilde{k}_{\perp} is the characteristic gluon transverse momentum in the absorptive ladder. The characteristic \tilde{k}_{\perp}^2 increases with energy, and $\lambda \approx 0.2 - 0.25$ at $Q^2 = 4 \text{ GeV}^2$ [47, 48]. Ultimately, the amplitude of the additional interaction would thus reach a strength comparable to the maximal one (BDL), resulting in complete suppression of RGS.

A semi-realistic estimate, using the eikonal approximation for the scattering of the colorless dipoles and assuming $\lambda \approx 0.2 - 0.25$, suggests that at the LHC energy the additional suppression is significant (a factor 2–3) for Higgs boson production by valence gluons, but much less so for processes initiated by valence quarks; at the Tevatron energy the effect should be much less pronounced for both gluons and quarks. In order to evaluate this additional suppression at LHC energies quantitatively, one

needs to follow the space–time evolution of the production of small- x , large-virtuality partons, and must not restrict the discussion to the gluon GPDs in the individual protons.

We emphasize that the screening effect described here is not included in the definition of the RGS probability due to soft interactions, as it corresponds to a modification of the probability of finding two gluons at small transverse distances without reference to the spectator interactions. Detailed calculations of the RGS probability including this effect require modeling of the color connections in the parton wavefunctions of the protons. Another perturbative screening correction to the hard process, due to diffraction into high-mass states (with the mass increasing with the collision energy) was considered in Ref. [49], which leads to a complementary suppression of the amplitude for exclusive double-gap diffraction.

B. Correlations between hard and soft interactions

In our treatment of RGS in Section IV B we have not taken into account effects due to correlations between partons in the wavefunctions of the colliding protons. Generally speaking, in the presence of such correlations the selection of particular configurations by the hard scattering process changes soft interactions as compared to “average” configurations. The neglect of this change is basic to the approximation (52), in which hard and soft interactions are assumed to commute also with respect to transverse degrees of freedom. A consistent treatment of correlation effects requires a much more detailed description of hard and soft interactions and the parton–hadron interface than the one given in Section IV. Here we would like to discuss this problem at the qualitative level, preparing the ground for a future in-depth investigation.

As a pedagogical example illustrating the effect of correlations on the RGS probability, let us consider double-gap diffractive proton–deuteron (pd) scattering — possibly including the quasi-elastic channel — within the framework of Eq. (77). The profile function for pd elastic scattering is significantly smaller than that for pp scattering even for energies at which pp scattering is close to the black-disk limit,

$$\Gamma^{dp} \ll \Gamma^{pp} \lesssim 1. \quad (84)$$

This follows from Eq. (3) when noting that the dp total cross section is approximately equal to twice the pp cross section, while the spatial size of the deuteron is much larger than the proton radius, and can be understood simply as the result of a “dilution” of the blackness of the individual protons due to their transverse motion in the deuteron bound state. At the same time, the transverse spatial distribution of gluons is now characterized by the transverse size of the deuteron. Because of Eq. (84), the factor $|1 - \Gamma^{dp}|^2$ in Eq. (77) is always of order unity, and no significant suppression takes place as it does in

pp scattering. Thus, one would conclude that the RGS probability is much larger in dp than in pp scattering, which is clearly nonsensical. The paradox is resolved by noting that hard and soft interactions in diffractive pd scattering are highly correlated. By considering events with a hard process one is effectively selecting configurations in which the projectile proton scatters from one of the nucleons. Soft interactions in these configurations are significantly larger than in pd scattering in average configurations, in which there is a substantial chance of the projectile “missing” the nucleons in the deuteron [67].

The deuteron example shows that transverse correlations in the wavefunctions can qualitatively change the picture of RGS. In particular, positive spatial correlations between hard partons and the opacity for soft interactions decrease the RGS probability compared to the uncorrelated estimate based on Eq. (77). In connection with pp scattering, Eq. (1), we now discuss the effects of two types of transverse correlations: (a) long-distance correlations due to scattering from the proton’s long-range pion field (“pion cloud”), (b) short-distance correlations related to parton clustering in “constituent quarks”.

A distinctive contribution to diffractive pp scattering at small $p'_{1\perp}$ results from the process in which a soft pion, emitted and absorbed by proton 1, scatters diffractively from proton 2. This contribution could properly be calculated using the known pion–nucleon coupling, and applying Eqs. (66)–(69) to the πp diffractive amplitude, with the two-gluon formfactor in the pion and the profile function of πp elastic scattering. It is generally small, for two reasons. First, the coupling of the soft pion to the nucleon is small because it is the Goldstone boson of spontaneously broken chiral symmetry. Second, softness of the pion implies that its longitudinal momentum fraction in the proton be small, $y \lesssim m_\pi/m_p$. In Higgs production at the LHC, where $x_{1,2} \sim 10^{-2}$, this puts the momentum fraction of the gluons in the pion at relatively large values, $z \sim x_{1,2}/y \sim 10^{-1}$, where the gluon distribution is not enhanced by DGLAP evolution.

In the partonic picture, the pion cloud contribution represents the result of specific correlations between hard and soft partons in the proton wavefunction. This observation has an interesting consequence for the estimate of the RGS probability for pp diffractive scattering based on Eq. (77). Namely, the gluon distribution in the proton receives a contribution from the pion cloud at transverse distances $\rho \sim 1/(2m_\pi)$ and momentum fractions $x \lesssim m_\pi/m_N$ [33]. Including this contribution in Eq. (77) would be inconsistent, since a hard process involving these gluons in the pion cloud should be accompanied by a very specific modification of the soft interactions, which is not accounted for in Eq. (77). For this reason, we have not included an explicit pion cloud contribution in the two-gluon formfactor parametrization used in our estimate leading to the value (83). More precisely, if we knew the “physical” gluon GPD, which by definition includes the pion cloud contribution, we would need to remove this contribution before using the GPD in Eq. (77), and

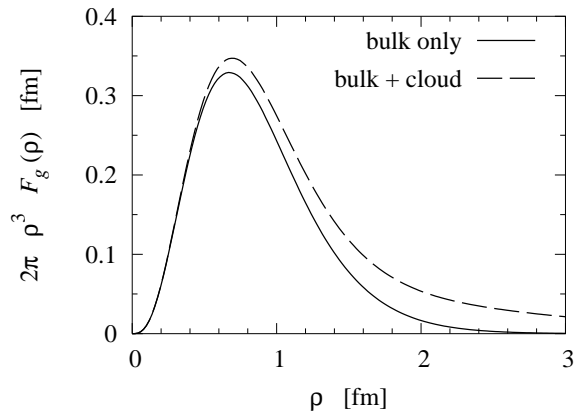


FIG. 12: The two-component parametrization of the transverse spatial distribution of gluons including the pion cloud, Eqs. (85) and (86). Shown are the radial distributions $2\pi\rho^3 F_g(\rho)$, the integral of which determines the average gluonic transverse size, $\langle\rho^2\rangle$. For the sake of comparison, the figure shows the combined (bulk + cloud) distribution without adjustment of the normalization factor ($N = 1$), so that the bulk contribution is the same as in the case of no pion cloud.

thus obtain a lower value for the RGS probability. This is just another example of the general rule that correlations lower the RGS probability compared to the independent interaction approximation, Eq. (77).

To estimate the correction resulting from the removal of the pion cloud contribution from the gluon GPD, we evaluate Eq. (77) with a “two-component” parametrization of the two-gluon formfactor (*viz.* the transverse spatial distribution of gluons) including the pion cloud. We write

$$F_g(\rho) = N [F_{\text{bulk}}(\rho) + F_{\text{cloud}}(\rho)], \quad (85)$$

where N is a factor which ensures overall normalization to $\int d^2\rho F_g(\rho) = 1$. The “bulk” contribution to the two-gluon formfactor we parametrize by the dipole formfactor with $m_g^2 = 1 \text{ GeV}^2$, Eq. (31), the “cloud” contribution as

$$F_{\text{cloud}}(\rho) = C_{\text{cloud}} \frac{\rho^2}{\rho^2 + \rho_0^2} \frac{e^{-2m_\pi\rho}}{2m_\pi\rho}. \quad (86)$$

This form is essentially the asymptotic form of the gluon density at $\rho \gtrsim 1/(2m_\pi)$ for $x \ll m_\pi/m_N$ (“Yukawa tail”) [33], regularized at small ρ such as to avoid a large contribution in the bulk region; the parameter ρ_0^2 is chosen of the order $\langle\rho^2\rangle_{g,\text{bulk}} = 8/m_g^2 = 0.3 \text{ fm}^2$. The coefficient C_{cloud} we determine such that the inclusion of the cloud contribution increases the overall gluonic transverse size of the proton by 30%, which is the value found in the calculation of Ref. [33] (based on the phenomenological gluon distribution in the pion) and supported by the J/ψ photoproduction data; see Section III. Figure 12 shows the transverse spatial distributions for “bulk only” and “bulk + cloud”, multiplied by $2\pi\rho^3$, the integral of which

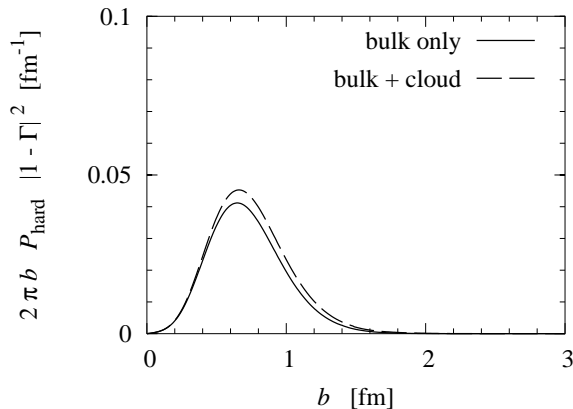


FIG. 13: The integrand (impact parameter distribution) in the rapidity gap survival probability, Eq. (77), for the two-component form of the transverse spatial distribution of gluons. The parameters are the same as in Fig. 12.

determines $\langle \rho^2 \rangle_g$. Figure 13 shows the impact parameter distributions in the RGS probability (*cf.* Fig. 8) obtained in the two cases. One sees that removal of the pion cloud contribution indeed reduces the RGS probability. The numerical effect turns out to be rather small,

$$\frac{S^2(\text{bulk only})}{S^2(\text{bulk + cloud})} = 0.94. \quad (87)$$

This can be explained by the fact that the pion cloud contribution to the gluon density is noticeable compared to the bulk only at transverse distances $\rho \gg 1/(2m_\pi) = 0.7 \text{ fm}$, while the RGS integral is dominated by rather short distances, $\rho_{\text{eff}} \sim b_{\text{eff}}/2 \sim 0.4 \text{ fm}$, *cf.* Figs. 7 and 8.

Corrections to the rapidity gap survival probability as given by Eq. (77) can also come from transverse short-distance correlations in the proton wavefunction (correlation length \ll proton size). The Tevatron CDF data on $\bar{p}p$ collisions with multiple hard processes (three jet plus photon production) [12] indicate the presence of significant correlations between the transverse positions of hard partons over distances $r \sim 0.3 \text{ fm}$ [10]. Given one hard parton with $x \gtrsim 0.05$ at a certain transverse position, it is much more likely to find in the proton wavefunction a second hard parton $x \gtrsim 0.05$ within a distance $\sim r$ than elsewhere in the transverse plane. As a result, in pp events with (at least) one hard process the probability for a second hard interaction is substantially larger (by a factor of ~ 2) than it would be without correlations. One may also suppose that the local cross section density (opacity) for soft inelastic interactions is higher near the position of a hard parton than elsewhere. Such correlations would result in a higher probability for inelastic interactions in pp events with a hard process (such as the hard two-gluon exchange in double-gap diffractive production) as compared to generic pp collisions, and would thus decrease the RGS probability compared to Eq. (77).

The corrections to Eq. (77) due to short-distance correlations can be viewed as an effective reduction of the

size of the diffractively scattering system, from the proton radius to the size of the transverse correlation, r . The corrections could be particularly large in the situation when the correlated areas are “black spots,” while the proton overall is still “gray” because of the dilution by the transverse motion. This situation would in a sense correspond to the above example of the deuteron, with the proton now playing the role of the deuteron. A quantitative description of these effects would require detailed modeling of the correlation between hard partons and the opacity for soft inelastic interactions, including an analysis of pp elastic scattering allowing local fluctuations in opacity, which are outside of the scope of the present paper.

A model of the proton accounting for short-distance correlations between partons is the so-called chiral quark-soliton model [52], which describes the proton as a system of constituent quarks bound by a classical pion field, see Ref. [53] for a review. This model implements the short-distance scale related to the spontaneous breaking of chiral symmetry, which appears here as the “size” of the constituent quark, $r \sim 0.3 \text{ fm}$ (in the Euclidean formulation of QCD this scale can be associated with the average instanton size in the vacuum). This model provides a consistent description of the twist-2 quark- and antiquark distributions in the nucleon at the scale $\mu \sim r^{-1} \approx 600 \text{ MeV}$ [55]. It also suggests that the gluons at this scale are “packaged” inside the constituent quarks and antiquarks [53]. Assuming perturbative QCD evolution to be applicable starting from this scale one would thus expect significant correlations between the positions of hard quarks and gluons and the opacity for soft interactions over a transverse size $r \sim 0.3 \text{ fm}$. Incorporating these correlations into the description of the BDL in high-energy pp scattering and the theory of RGS in diffractive processes is an important problem for future studies.

To summarize, the dynamical mechanisms which we have discussed here (and indeed all mechanism which we are aware of) give rise to positive correlations between the transverse position of hard partons and the opacity for inelastic interactions. We can thus say with some confidence that estimates based on the independent interaction approximation, Eq. (77), represent an upper bound on the RGS probability.

VII. TRANSVERSE MOMENTUM DEPENDENCE

The interplay of hard and soft interactions in exclusive double-gap diffraction not only causes the suppression of the integrated cross section summarized in the RGS probability, but also gives rise to a distinctive dependence of the cross section on the final proton transverse momenta. By observing this “diffraction pattern” one can perform detailed tests of the diffractive reaction mechanism, and even extract information about the two-gluon formfac-

tors of the colliding protons. The transverse momentum dependence also contains information about the quantum numbers (parity) of the produced system [5]. We consider here production of a 0^+ system, for which the hard scattering amplitude depends on the proton transverse momenta only through $|\mathbf{p}'_{1\perp}|$ and $|\mathbf{p}'_{2\perp}|$, and the diffractive amplitude is given by Eq. (66); we comment on production of 0^- systems at the end of this section.

For a quick orientation over the transverse momentum dependence, we evaluate the amplitude with the exponential parametrizations of the two-gluon formfactor, Eqs. (33), and the pp elastic scattering amplitude, Eq. (12). In this case the convolution integral in Eq. (66) reduces to a Gaussian integral, and we obtain a closed expression for the amplitude,

$$T_{\text{diff}}(\mathbf{p}'_{1\perp}, \mathbf{p}'_{2\perp}) = \kappa \exp\left(-\frac{B_{g1}\mathbf{p}'_{1\perp}{}^2}{2} - \frac{B_{g2}\mathbf{p}'_{2\perp}{}^2}{2}\right) \times \left\{1 - \frac{B}{B_{\text{tot}}} \exp\left[\frac{(B_{g1}\mathbf{p}'_{1\perp} - B_{g2}\mathbf{p}'_{2\perp})^2}{2B_{\text{tot}}}\right]\right\}, \quad (88)$$

where $B_{g1} \equiv B_g(x_1)$ and $B_{g2} \equiv B_g(x_2)$ are the slopes corresponding to the momentum fractions $x_{1,2} \sim \xi_{1,2}$, and

$$B_{\text{tot}} \equiv B_{g1} + B_{g2} + B. \quad (89)$$

[As a check, we note that the integral of the square of this expression, divided by the corresponding expression for $B = 0$ (no soft interactions), reproduces the result for the RGS probability obtained in the coordinate space calculation, Eq. (81).] The amplitude (88) vanishes trivially for large $|\mathbf{p}_{1\perp}|$ or $|\mathbf{p}_{2\perp}|$, independently of the directions of the momentum vectors. In addition, it has a zero at finite values of the transverse momenta, namely at

$$(B_{g1}\mathbf{p}'_{1\perp} - B_{g2}\mathbf{p}'_{2\perp})^2 = 2B_{\text{tot}} \ln \frac{B_{\text{tot}}}{B} \approx 2(B_{g1} + B_{g2}) \quad (B \gg B_{g1}, B_{g2}). \quad (90)$$

This zero arises because of the destructive interference of the amplitude of the hard scattering process alone and the amplitude including soft elastic rescattering, *cf.* Fig. 6, and directly reflects the interplay of hard and soft interactions. It leads to a dip in the diffractive cross section, and thus to a typical “diffraction pattern” in the dependence on the transverse momentum of the first proton, $\mathbf{p}'_{1\perp}$, at fixed transverse momentum of the second proton, $\mathbf{p}'_{2\perp}$. Figure 14 shows this diffraction pattern in the kinematics of Higgs production at the LHC at zero rapidity, for which $B_{g1} = B_{g2}$. One sees that the pattern in $\mathbf{p}'_{2\perp}$ evolves from a rotationally symmetric one for $\mathbf{p}'_{1\perp} = 0$ to a two-centered one for large $|\mathbf{p}'_{1\perp}|$. This basic feature of the diffractive cross section does not depend on the details of the parametrization of the

two-gluon formfactor; similar results are obtained with the dipole parametrization, *cf.* the detailed comparison below.

The diffraction pattern of Fig. 14 implies a strong angular dependence of the cross section, which, moreover, changes with the magnitude of the transverse momenta, $|\mathbf{p}'_{1\perp}|$ and $|\mathbf{p}'_{2\perp}|$. This is illustrated in Figure 15, which shows the dependence of $|T_{\text{diff}}|^2$ on the angle between the transverse momenta, ϕ , for various values of $|\mathbf{p}'_{1\perp}| = |\mathbf{p}'_{2\perp}|$. For small values of the transverse momenta the cross section is maximal at zero angle; for large values (where the cross sections as a function of angle runs through the diffractive dip) it is maximal at $\phi = \pi$. This dependence needs to be taken into account when attempting to maximize the diffractive cross section in the search for new particles.

An interesting question is which specific features of the transverse momentum dependence of the diffractive cross section could be used to test the diffractive reaction mechanism, and possibly extract information about the two-gluon formfactors of the colliding protons. Such studies would be feasible in diffractive dijet production, which has a relatively large cross section and also allows one to vary the invariant mass of the diffractively produced system, and thus the effective values of the gluon momentum fraction, x_1 and x_2 . To address this question, we again start from the explicit expression for the amplitude obtained with the exponential parametrization of the two-gluon formfactor, Eq. (88). We rewrite it in terms of the center-of-mass and relative transverse momenta of the final-state protons,

$$\begin{aligned} \mathbf{P}_\perp &\equiv (\mathbf{p}'_{1\perp} + \mathbf{p}'_{2\perp})/2, \\ \mathbf{r}_\perp &\equiv \mathbf{p}'_{1\perp} - \mathbf{p}'_{2\perp}, \end{aligned} \quad (91)$$

and obtain

$$T_{\text{diff}}(\mathbf{p}'_{1\perp}, \mathbf{p}'_{2\perp}) = \kappa \exp\left[-\frac{B_{g1} + B_{g2}}{2} \left(\mathbf{P}_\perp^2 + \frac{\mathbf{r}_\perp^2}{4}\right) - \frac{B_{g1} - B_{g2}}{2} (\mathbf{P}_\perp \mathbf{r}_\perp)\right] \times \left\{1 - \frac{B}{B_{\text{tot}}} \exp\left[\frac{(B_{g1} - B_{g2})^2}{2B_{\text{tot}}} \mathbf{P}_\perp^2 + \frac{(B_{g1} + B_{g2})^2}{2B_{\text{tot}}} \frac{\mathbf{r}_\perp^2}{4} + \frac{(B_{g1} - B_{g2})(B_{g1} + B_{g2})}{2B_{\text{tot}}} (\mathbf{P}_\perp \mathbf{r}_\perp)\right]\right\}. \quad (92)$$

For production at zero rapidity, for which $x_1 = x_2 \equiv x$,

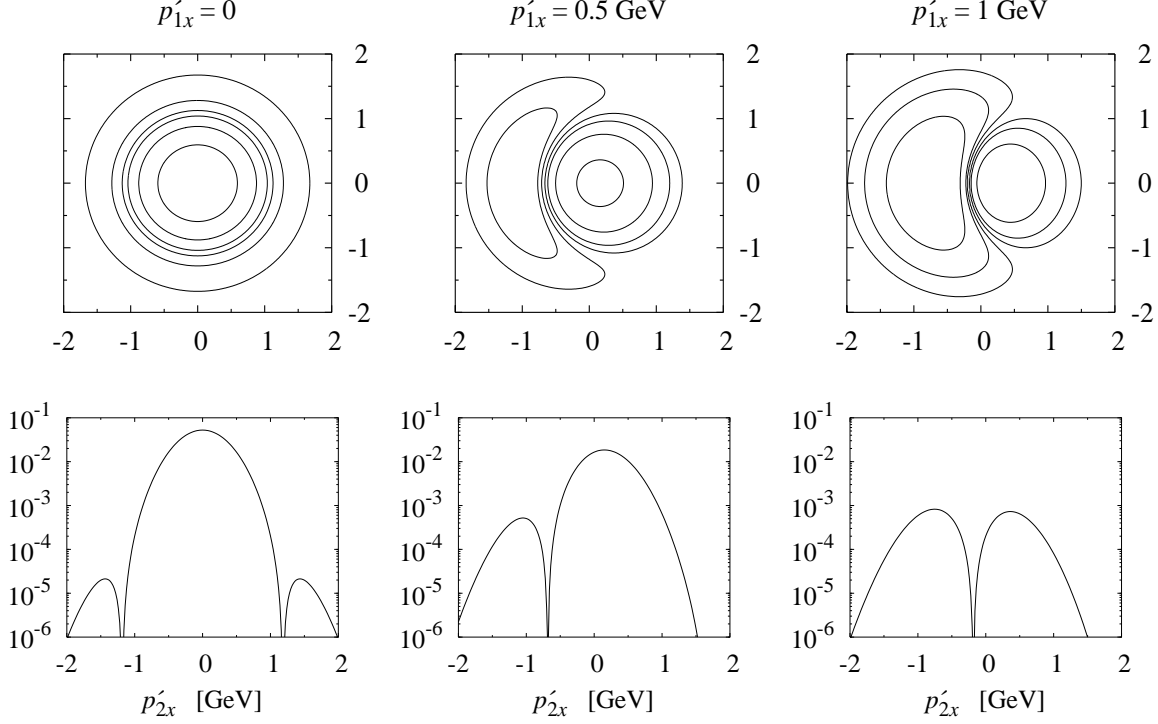


FIG. 14: Transverse momentum dependence of the cross section for double-gap exclusive diffraction (1). The plots show the modulus squared of the amplitude, $|T_{\text{diff}}|^2$, with $\kappa = 1$, as a function of $\mathbf{p}'_{2\perp}$, for three fixed values of $\mathbf{p}'_{1\perp}$ (chosen to point in x -direction, $p'_{1y} = 0$). The upper row of plots show the contours of constant values of $|T_{\text{diff}}|^2$ on a logarithmic scale as functions of p'_{2x} and p'_{2y} (in units of GeV). The lower row of plots shows the profile along the $p'_{2y} = 0$ axis. Shown are the results calculated with the exponential parametrizations of the two-gluon formfactor and the pp elastic amplitude, Eq. (88). The diffraction pattern in $\mathbf{p}'_{2\perp}$ evolves from a rotationally symmetric one for $\mathbf{p}'_{1\perp} = 0$ to a two-centered one for large $|\mathbf{p}'_{1\perp}|$.

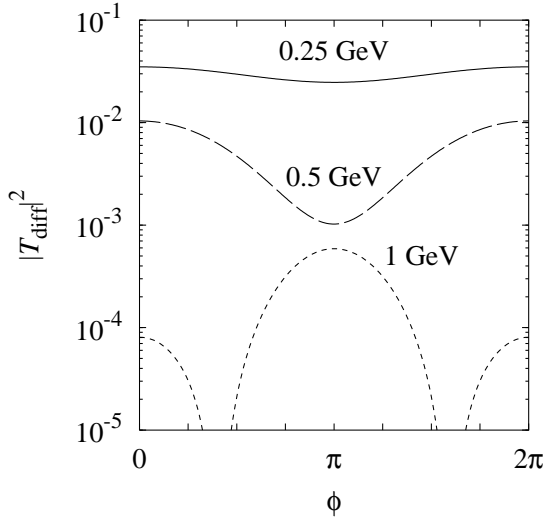


FIG. 15: Angular dependence of the cross section for double-gap diffractive production of a 0^+ system. The plot shows the modulus squared of the amplitude, $|T_{\text{diff}}|^2$, Eq. (66), with $\kappa = 1$. The numbers above the curves indicate the values of $|\mathbf{p}'_{1\perp}| = |\mathbf{p}'_{2\perp}|$. The kinematics corresponds to Higgs boson production at the LHC.

and $B_{g1} = B_{g2} \equiv B_g$, this simplifies to

$$\begin{aligned}
 T_{\text{diff}}(\mathbf{p}'_{1\perp}, \mathbf{p}'_{2\perp}) &= \exp\left(-B_g \mathbf{P}_\perp^2 - \frac{B_g \mathbf{r}_\perp^2}{4}\right) \\
 &\times \left[1 - \frac{B}{B_{\text{tot}}} \exp\left(\frac{B_g^2}{B_{\text{tot}}} \mathbf{r}_\perp^2\right)\right], \quad (93)
 \end{aligned}$$

where now $B_{\text{tot}} = B + 2B_g$. In this case the amplitude does not depend on the variable $(\mathbf{P}_\perp \mathbf{r}_\perp) = (\mathbf{p}'_{1\perp} - \mathbf{p}'_{2\perp})/2$, which is an obvious consequence of its symmetry with respect to the interchange of $\mathbf{p}'_{1\perp}$ and $\mathbf{p}'_{2\perp}$. Furthermore, one sees that the dependences of Eq. (93) on \mathbf{P}_\perp^2 and \mathbf{r}_\perp^2 are very different. The dependence on \mathbf{P}_\perp^2 is monotonic and governed by the parameter B_g alone; it essentially probes the square of the two-gluon formfactors of the colliding protons. The dependence on \mathbf{r}_\perp^2 , however, is governed by both B_g and B , and exhibits the diffractive zero (90); it reflects the interplay of hard and soft interactions.

The qualitative differences between the \mathbf{P}_\perp and \mathbf{r}_\perp dependence of the amplitude are not specific to the exponential parametrization of the two-gluon formfactor, and

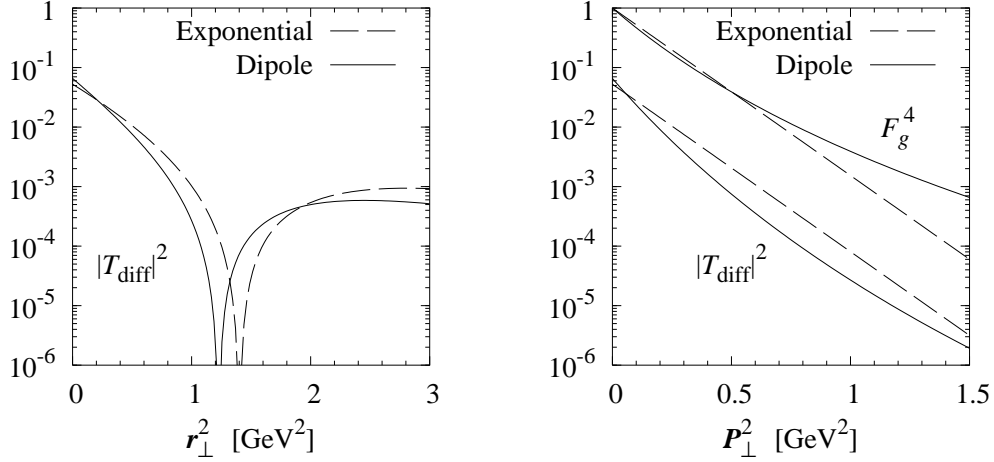


FIG. 16: *Left*: Dependence of the cross section for double-gap diffractive 0^+ production on the square of the difference of the proton transverse momenta, r_\perp^2 , for $\mathbf{P}_\perp = 0$ (*i.e.*, $\mathbf{p}'_{1\perp} = -\mathbf{p}'_{2\perp} = 2\mathbf{r}_\perp$). The kinematics corresponds to production of a system with $M = 140$ GeV at the LHC energy at zero rapidity ($x_1 = x_2 \sim 10^{-2}$). The plot shows the modulus squared of the amplitude, $|T_{\text{diff}}|^2$, Eq. (66), with $\kappa = 1$, obtained with the exponential and dipole parametrizations of the two-gluon formfactor. For the exponential parametrization, the position of the diffractive zero is given by Eq. (90). *Right*: Dependence on the square of the sum of the transverse momenta, \mathbf{P}_\perp^2 , for $\mathbf{r}_\perp = 0$ (*i.e.*, $\mathbf{p}'_{1\perp} = \mathbf{p}'_{2\perp} = \mathbf{P}_\perp$). Also shown is $F_g^4(t)$ for the two parametrizations, which would be the t -dependence of the amplitude without soft spectator interactions.

can be used to test the diffractive reaction mechanism and extract information about the two-gluon formfactor. Figure 16 (left plot) shows the squared modulus of the amplitude (for $\kappa = 1$) as a function of r_\perp^2 , for $\mathbf{P}_\perp = 0$, in the kinematics corresponding to dijet production with $x = 10^{-2}$ at the LHC. One sees that the dependence in the forward peak (near $r_\perp^2 = 0$), and even the position of the diffractive dip, are not very different for the two parametrizations. Experimental observation of this structure would thus constitute a stringent test of the diffractive reaction mechanism.

Figure 16 (right plot) shows the dependence of the cross section for double-gap diffractive 0^+ production on \mathbf{P}_\perp^2 , for $\mathbf{r}_\perp = 0$. Also shown is the fourth power of the two-gluon formfactor, $F_g^4(t)$ for the two parametrizations, which would be the t -dependence of the amplitude without soft spectator interactions. For the exponential parametrization the t -dependence of the full diffractive amplitude is identical to that of $F_g^4(t)$, *cf.* Eqs. (93) and (33); one sees that the two dependences are similar also for the dipole parametrization. The different normalization of the two sets of curves reflects the RGS probability, *cf.* Sec. V A.

The position of the diffractive zero in the r_\perp^2 -dependence (see Fig. 16, left plot) is correlated with the slope of the monotonic \mathbf{P}_\perp^2 -dependence of the diffractive cross section; both essentially reflect the two-gluon formfactor of the colliding protons. A sensible strategy for the analysis of double-gap diffractive dijet production would be to first establish the existence of the diffractive zero in r_\perp^2 at $\mathbf{P}_\perp = 0$, and then extract B_g from the \mathbf{P}_\perp^2 -dependence of the diffractive cross section at $\mathbf{r}_\perp = 0$, where the cross section is maximal. In the next step,

one could change the dijet mass (*i.e.*, the momentum fractions $x_1 = x_2 = x$ in the two-gluon formfactor) and verify whether both the position of the zero and the \mathbf{P}_\perp^2 -slope change proportionately, and whether the rate of change with $\ln x$ is consistent with the value of α'_g at the relevant scale, *cf.* Eq. (27).

The $x_{1,2}$ -dependence of the two-gluon formfactor in the protons can be probed more directly by extending the measurements of diffractive production to non-zero rapidity, $y \neq 0$, corresponding to different momentum fractions of the annihilating gluons in the two protons,

$$x_{1,2} = x e^{\pm y}, \quad x \equiv \frac{m_H}{\sqrt{s}}. \quad (94)$$

In this case the two-gluon formfactors of the two protons are different, and the diffractive cross section is no longer invariant under exchange of the final proton transverse momenta, $\mathbf{p}'_{1\perp} \leftrightarrow \mathbf{p}'_{2\perp}$. One sees that the expression for the amplitude obtained with the exponential parametrization, Eq. (93), acquires a dependence on $(\mathbf{P}_\perp \mathbf{r}_\perp) = (\mathbf{p}'_{1\perp} - \mathbf{p}'_{2\perp})/2$, which is controlled by the difference of the slopes, $B_{g1} - B_{g2}$. With the x -dependence of the individual slopes given by

$$B_{g1} \equiv B_g(x_1) = B_g(x) + 2\alpha'_g \ln \frac{x_1}{x}, \quad (95)$$

$$B_{g2} \equiv B_g(x_2) = B_g(x) + 2\alpha'_g \ln \frac{x_2}{x}, \quad (96)$$

their difference is directly proportional to the rapidity [*cf.* Eq. (94)],

$$B_{g1} - B_{g2} = 2\alpha'_g y. \quad (97)$$

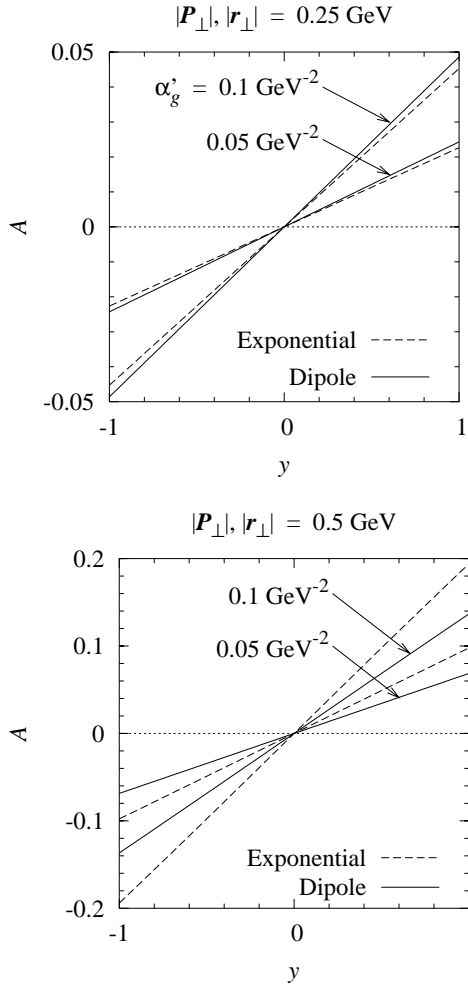


FIG. 17: The cross section asymmetry (98) as a function of rapidity, y . Shown are the results obtained with the exponential and the dipole parametrizations of the two-gluon formfactor, for two representative values of α'_g . In this calculation only the y -dependence of the cross section arising from the convolution integral is taken into account, not the y -dependence arising from the overall normalization, κ .

For small rapidities, $|y| \lesssim 1$, and because of the relatively small value of α'_g this difference is substantially smaller than the central value, $B_g(x)$, and the dependence of the amplitude on $(\mathbf{P}_\perp \mathbf{r}_\perp)$ can be treated in first-order approximation. This implies that the cross section depends practically linearly on $(\mathbf{P}_\perp \mathbf{r}_\perp)$ for $|y| \lesssim 1$.

A convenient observable to measure is the asymmetry of the cross section with respect to $\mathbf{r}_\perp \rightarrow -\mathbf{r}_\perp$ and $\mathbf{P}_\perp \rightarrow \mathbf{P}_\perp$ (i.e., $\mathbf{p}'_{1\perp} \leftrightarrow \mathbf{p}'_{2\perp}$) at fixed x and $y \neq 0$ (i.e., fixed $x_1 \neq x_2$),

$$A \equiv \frac{\sigma_{\text{diff}}(\mathbf{p}'_{1\perp}, \mathbf{p}'_{2\perp}) - \sigma_{\text{diff}}(\mathbf{p}'_{2\perp}, \mathbf{p}'_{1\perp})}{\sigma_{\text{diff}}(\mathbf{p}'_{1\perp}, \mathbf{p}'_{2\perp}) + \sigma_{\text{diff}}(\mathbf{p}'_{2\perp}, \mathbf{p}'_{1\perp})}; \quad (98)$$

alternatively, one could exchange the rapidities and leave the transverse momenta the same. This asymmetry is odd in y and vanishes linearly for $y \rightarrow 0$. For $|y| \lesssim 1$, it is

practically is proportional to $(\mathbf{P}_\perp \mathbf{r}_\perp) = (\mathbf{p}'_{1\perp} - \mathbf{p}'_{2\perp})/2$. When calculating the asymmetry at finite y , we have to take into account that, in general, also the overall normalization of the cross section, $\kappa(s, \xi_1, \xi_2)$, changes with y , because of the change of arguments in the $t = 0$ gluon GPDs of the protons, see Eq. (62). However, this change relative to the value at $y = 0$ is of second order in y (the changes in the arguments of the gluon densities cancel each other to first order) and can be neglected for small y . This implies that for $y \ll 1$, the asymmetry is of the form

$$A \sim C y \alpha'_g(\mathbf{P}_\perp \mathbf{r}_\perp), \quad (99)$$

where the constant, C , is calculable solely from the convolution integral of the two-gluon formfactor and the pp elastic amplitude, and does not contain information on the gluon densities. For finite y , the asymmetry is still proportional to $\alpha'_g(\mathbf{P}_\perp \mathbf{r}_\perp)$, but the coefficient is a more complicated function of y , which depends also on the gluon densities in the colliding protons. Figure 17 shows the theoretical estimate of the asymmetry as obtained with the exponential and the dipole parametrizations of the two-gluon formfactor, as a function of the rapidity, y , for two representative values of α'_g . In this calculation, for simplicity, we have taken into account only the y -dependence of the cross section arising from the RGS integral, not the y -dependence arising from the overall normalization, κ . The latter is $\propto y^2$ at small y but may be numerically important at $y \sim 1$; the curves in this region are shown for illustrative purposes only.

In the above discussions we have considered production of a 0^+ system. The cross section for production of a 0^- state is significantly suppressed compared to 0^+ . This is because in the hard scattering process only one gluon polarization state gives a large contribution in the LO approximation [44], and from one gluon polarization it is impossible to build a parity-conserving amplitude for the production of a 0^- state.

Our discussion of the transverse momentum dependence in this Section is based on the approximation of independent hard and soft interactions, Eqs. (66–70). One should expect that the inclusion of correlations between hard and soft interactions, as described in Section VI, would modify not only the RGS probability but also the transverse momentum dependence of double-gap exclusive diffraction. This interesting question will be addressed elsewhere.

VIII. DISCUSSION AND OUTLOOK

In this paper we have outlined an approach to RGS in double-gap exclusive diffractive processes in pp scattering based on the idea that hard and soft interactions are approximately independent because they proceed over widely different time- and distance scales. We have shown that this idea can be practically implemented

in the framework of Gribov’s parton picture of high-energy scattering, and gives rise to a conceptually clear and quantitative description of RGS.

In the independent interaction approximation, where correlations between hard and soft interactions are neglected, the RGS probability can be expressed in a model-independent fashion in terms in two phenomenological ingredients — the gluon GPD in the proton, and the pp elastic scattering amplitude. At this level we recover a simple geometric picture of the interplay of hard and soft interactions in the impact parameter representation. The fact that the pp elastic amplitude at high energies approaches the BDL at TeV energies suppresses small impact parameters and ensures dominance of peripheral scattering in double-gap diffraction. This is crucial both for justifying the approximations made in our derivation, and for determining the numerical value of the RGS probability. Our numerical results for the RGS probability are somewhat lower than those obtained previously within the eikonalized Pomeron model of soft interactions; the agreement of Eq. (83) with the best estimate quoted in Ref. [5] is accidental and due to the fact that these authors assume a larger radius of the transverse spatial distribution of gluons with $x \sim 10^{-2}$.

Our numerical prediction for the RGS probability in double-gap exclusive diffractive Higgs boson production at the LHC ($m_H = 100 - 200$ GeV, $\sqrt{s} = 14$ TeV) in the independent interaction approximation is $S^2 \approx 0.03$. According to the detailed calculations of Ref. [5], this would put the estimated cross section for Higgs production in the minimal supersymmetric model (MSSM) with detection through the $b\bar{b}$ mode at $\text{Br}(H \rightarrow b\bar{b}) \sigma_{\text{diff}}(0^+) \sim \text{few} \times 10 \text{ fb}$, which should be accessible at the LHC; see Ref. [5] for details.

Our partonic approach to RGS also allows us to discuss the effect of correlations between hard and soft interactions on the RGS probability. Such correlations lower the RGS probability compared to the independent interaction approximation. In the case of long-distance correlations due to the proton’s pion cloud, we estimated this effect to be of the order of $\sim 10\%$. Potentially more important are short-distance correlations, *e.g.* those suggested by the phenomenological concept of a “constituent quark” structure of the proton). Such correlations can be regarded as a change of the effective size of the diffractively scattering systems, and could reduce the predictions for the RGS probability by a substantial factor. In view of its importance for the Higgs boson search at the LHC this problem clearly requires further theoretical study. It can in principle also be addressed experimentally, by “measuring” the RGS probability in double-gap processes for which the hard scattering amplitude is known, such as dijet production.

An important ingredient in our description of RGS is the profile function of the complex pp elastic scattering amplitude. This underscores the importance of the planned measurements of pp elastic scattering and total cross sections in the TOTEM experiment at the LHC

[56], as well as at RHIC [57]. In addition to providing input for more accurate estimates of the RGS probability in diffraction, such measurements would allow us to further explore the fascinating new regime of the BDL in high-energy hadron-hadron scattering.

Measurements of the transverse momentum dependence of double-gap exclusive diffractive processes with large cross section (dijet production) would allow one to perform detailed studies of the diffractive reaction mechanism. Following the strategy outlined in Section VII, once the reaction mechanism has been established, one could even use such processes to extract information about the transverse spatial distribution of gluons in the colliding protons, including its change with x . Such studies would complement the information on the two-gluon formfactor obtained from vector meson production at HERA or a future electron-ion collider (EIC). Eventually, using QCD evolution as well as models of nucleon structure, these data on the transverse spatial distribution of gluons could also be correlated with the planned measurements of quark GPDs in hard exclusive processes in ep scattering in fixed-target experiments (HERMES, JLab 12 GeV, COMPASS). One of the advantages of Gribov’s parton picture of hard and soft interactions is precisely that it unifies the description of hadron-hadron and electron/photon-hadron scattering at high energies. Other ways to probe GPDs in pp scattering with hard processes (non-diffractive) have been described in Ref. [10].

We would like to comment on some of the experimental aspects of measurements of the transverse momentum dependence of double-gap exclusive diffraction with the proposed forward detectors at the LHC. Such measurements require good energy resolution in order to guarantee exclusivity and determine the mass of the diffractively produced system, as well as sufficient transverse momentum resolution to map the $\mathbf{p}_{1\perp}, \mathbf{p}_{2\perp}$ distributions. An important experimental problem is that the intrinsic transverse momentum distribution in the beams at the interaction point (IP) puts a lower bound on the transverse momentum transfers that can be resolved. This distribution is determined by the beam optics, and thus closely correlated with the luminosity. The proposed 420 m forward detectors for the CMS and ATLAS experiments [13, 58] can tag protons in the range $0.002 \leq \xi \leq 0.015$; in the TOTEM experiment at CMS with detectors at 200 m the range will be extended to $\xi < 0.1$ [59]. Both detectors can obtain a longitudinal and transverse momentum resolution comparable to the beam distributions. At a luminosity of $10^{33} \text{ cm}^{-2} \text{ s}^{-1}$ with $\beta^* = 0.5 \text{ m}$, and a one-sigma normalized emittance $\epsilon = 3.75 \times 10^{-6} \pi \text{ m}$, the one-sigma angular spread of the beams at the IP is $8 \mu\text{r}$, corresponding to a transverse momentum spread of $56 \text{ MeV}/c$. This sets the scale for experimental smearing of the transverse momentum distributions. The TOTEM experiment also envisages running at substantially larger β^* values (18, 90 and 1540 m). These values will reduce the transverse angular spread of the beams at the IP by $\sqrt{\epsilon/(\pi\beta^*)}$, but

with a concomitant reduction in luminosity. Given that the typical scale of the transverse momentum distributions is $m_g \approx 1$ GeV, it seems feasible to make detailed and precise measurements of the transverse momentum distributions with the LHC420 and TOTEM detectors even when running in high-luminosity mode.

Acknowledgments

We thank V. Khoze, R. Orava, and M. Ryskin for useful discussions. M. Ryskin kindly made available to us a

numerical parametrization of the pp elastic amplitude of Ref. [4].

Notice: Authored by Jefferson Science Associates, LLC under U.S. DOE Contract No. DE-AC05-06OR23177. The U.S. Government retains a non-exclusive, paid-up, irrevocable, world-wide license to publish or reproduce this manuscript for U.S. Government purposes. Supported by other DOE contracts and the Binational Science Foundation (BSF).

-
- [1] A. Schafer, O. Nachtmann and R. Schopf, Phys. Lett. B **249**, 331 (1990).
 - [2] A. Bialas and P. V. Landshoff, Phys. Lett. B **256**, 540 (1991).
 - [3] Y. L. Dokshitzer, V. A. Khoze and T. Sjostrand, Phys. Lett. B **274**, 116 (1992).
 - [4] V. A. Khoze, A. D. Martin and M. G. Ryskin, Eur. Phys. J. C **18**, 167 (2000) [arXiv:hep-ph/0007359].
 - [5] A. B. Kaidalov, V. A. Khoze, A. D. Martin and M. G. Ryskin, Eur. Phys. J. C **31**, 387 (2003) [arXiv:hep-ph/0307064].
 - [6] S. Nussinov, private communication to L. F.
 - [7] J. D. Bjorken, Phys. Rev. D **47**, 101 (1993).
 - [8] V. N. Gribov, arXiv:hep-ph/0006158.
 - [9] L. Frankfurt, M. Strikman and C. Weiss, Ann. Rev. Nucl. Part. Sci. **55**, 403 (2005) [arXiv:hep-ph/0507286].
 - [10] L. Frankfurt, M. Strikman and C. Weiss, Annalen Phys. **13**, 665 (2004) [arXiv:hep-ph/0410307].
 - [11] L. Frankfurt, M. Strikman, C. Weiss and M. Zhalov, arXiv:hep-ph/0412260.
 - [12] F. Abe *et al.* [CDF Collaboration], Phys. Rev. Lett. **79**, 584 (1997). F. Abe *et al.* [CDF Collaboration], Phys. Rev. D **56**, 3811 (1997).
 - [13] M. G. Albrow *et al.*, CERN-LHCC-2005-025
 - [14] M. G. Albrow *et al.*, arXiv:hep-ex/0511057.
 - [15] M. M. Block, E. M. Gregores, F. Halzen and G. Pancheri, Phys. Rev. D **60**, 054024 (1999) [arXiv:hep-ph/9809403].
 - [16] C. Bourrely, J. Soffer and T. T. Wu, Eur. Phys. J. C **28**, 97 (2003) [arXiv:hep-ph/0210264].
 - [17] M. M. Islam, R. J. Luddy and A. V. Prokudin, Mod. Phys. Lett. A **18**, 743 (2003).
 - [18] L. Frankfurt, M. Strikman and C. Weiss, Phys. Rev. D **69**, 114010 (2004) [arXiv:hep-ph/0311231].
 - [19] A. Martin, Phys. Rev. **129**, 1432 (1963).
 - [20] G. Marchesini and E. Rabinovici, Nucl. Phys. B **120**, 253 (1977); G. Marchesini, E. Rabinovici and L. Trentadue, Nucl. Phys. B **147**, 41 (1979).
 - [21] M. Diehl, Phys. Rept. **388**, 41 (2003) [arXiv:hep-ph/0307382].
 - [22] A. V. Belitsky and A. V. Radyushkin, Phys. Rept. **418**, 1 (2005) [arXiv:hep-ph/0504030].
 - [23] L. Frankfurt, A. Freund, V. Guzey and M. Strikman, Phys. Lett. B **418**, 345 (1998) [Erratum-ibid. B **429**, 414 (1998)] [arXiv:hep-ph/9703449].
 - [24] A. G. Shuvaev, K. J. Golec-Biernat, A. D. Martin and M. G. Ryskin, Phys. Rev. D **60**, 014015 (1999) [arXiv:hep-ph/9902410].
 - [25] M. Burkardt, Int. J. Mod. Phys. A **18**, 173 (2003).
 - [26] P. V. Pobylitsa, Phys. Rev. D **66**, 094002 (2002).
 - [27] M. Diehl, Eur. Phys. J. C **25**, 223 (2002).
 - [28] M. Binkley *et al.*, Phys. Rev. Lett. **48**, 73 (1982).
 - [29] A. Aktas *et al.* [H1 Collaboration], arXiv:hep-ex/0510016.
 - [30] S. Chekanov *et al.* [ZEUS Collaboration], Nucl. Phys. B **695**, 3 (2004) [arXiv:hep-ex/0404008].
 - [31] L. Frankfurt and M. Strikman, Phys. Rev. D **66** (2002) 031502.
 - [32] M. Strikman and C. Weiss, in Proceedings of the XII International Workshop on Deep Inelastic Scattering (DIS 2004), Strbske Pleso, Slovakia, Apr. 14-18, 2004 [arXiv:hep-ph/0408345].
 - [33] M. Strikman and C. Weiss, Phys. Rev. D **69**, 054012 (2004) [arXiv:hep-ph/0308191].
 - [34] J. F. Gunion, H. E. Haber, G. L. Kane and S. Dawson, "The Higgs hunter's guide," Frontiers in Physics, 80, Addison-Wesley (1990); Errata arXiv:hep-ph/9302272.
 - [35] V. A. Khoze, A. D. Martin and M. G. Ryskin, Phys. Lett. B **401**, 330 (1997) [arXiv:hep-ph/9701419].
 - [36] V. A. Khoze, A. D. Martin and M. G. Ryskin, Eur. Phys. J. C **14**, 525 (2000) [arXiv:hep-ph/0002072].
 - [37] S. J. Brodsky, L. Frankfurt, J. F. Gunion, A. H. Mueller and M. Strikman, Phys. Rev. D **50**, 3134 (1994) [arXiv:hep-ph/9402283].
 - [38] D. Mueller, D. Robaschik, B. Geyer, F. M. Dittes and J. Horejsi, Fortsch. Phys. **42**, 101 (1994) [arXiv:hep-ph/9812448].
 - [39] H. Abramowicz, L. Frankfurt and M. Strikman, Surveys High Energ. Phys. **11**, 51 (1997) [arXiv:hep-ph/9503437].
 - [40] X. D. Ji, Phys. Rev. D **55**, 7114 (1997) [arXiv:hep-ph/9609381].
 - [41] A. V. Radyushkin, Phys. Rev. D **56**, 5524 (1997) [arXiv:hep-ph/9704207].
 - [42] J. C. Collins and A. Freund, Phys. Rev. D **59**, 074009 (1999) [arXiv:hep-ph/9801262].
 - [43] G. P. Salam, arXiv:hep-ph/0501097.
 - [44] V. N. Gribov, "The theory of complex angular momenta: Gribov lectures on theoretical physics," Cambridge University Press, Cambridge, UK (2003).
 - [45] K. Goulianos, in: Proceedings of the 11th International Conference on Elastic and Diffractive Scattering: Towards High Energy Frontiers: The 20th Anniversary of the Blois Workshops, Chateau de Blois, Blois, France,

- 15–20 May 2005, arXiv:hep-ph/0510035.
- [46] L. D. Landau and E. M. Lifshits, in: *Course of Theoretical Physics, Vol. III: Quantum Mechanics*, Pergamon Press, Oxford, 1973.
 - [47] M. Ciafaloni, D. Colferai, G. P. Salam and A. M. Stasto, *Phys. Rev. D* **68**, 114003 (2003) [arXiv:hep-ph/0307188].
 - [48] G. Altarelli, R. D. Ball and S. Forte, *Nucl. Phys. B* **674**, 459 (2003) [arXiv:hep-ph/0306156].
 - [49] J. Bartels, S. Bondarenko, K. Kutak and L. Motyka, *Phys. Rev. D* **73**, 093004 (2006) [arXiv:hep-ph/0601128].
 - [50] M. L. Good and W. D. Walker, *Phys. Rev.* **120**, 1857 (1960).
 - [51] H. I. Miettinen and J. Pumplin, *Phys. Rev. D* **18**, 1696 (1978).
 - [52] D. Diakonov, V. Y. Petrov and P. V. Pobylitsa, *Nucl. Phys. B* **306**, 809 (1988).
 - [53] D. Diakonov, *Prog. Part. Nucl. Phys.* **51**, 173 (2003) [arXiv:hep-ph/0212026].
 - [54] T. Schafer and E. V. Shuryak, *Rev. Mod. Phys.* **70**, 323 (1998) [arXiv:hep-ph/9610451].
 - [55] D. Diakonov, V. Petrov, P. Pobylitsa, M. V. Polyakov and C. Weiss, *Nucl. Phys. B* **480**, 341 (1996) [arXiv:hep-ph/9606314]; *Phys. Rev. D* **56**, 4069 (1997) [arXiv:hep-ph/9703420].
 - [56] TOTEM Collaboration, CERN-LHCC-1997-049
 - [57] S. Bultmann *et al.*, *Phys. Lett. B* **632**, 167 (2006) [arXiv:nucl-ex/0507030]; S. L. Bultmann *et al.*, *Phys. Lett. B* **579**, 245 (2004) [arXiv:nucl-ex/0305012]; H. Spinka *et al.*, “Physics with Tagged Forward Protons with the STAR Detector at RHIC,” proposal to STAR, unpublished, June 8, 2005.
 - [58] B. Cox, Talk presented at XIV International Workshop on Deep Inelastic Scattering (DIS2006), Tsukuba City, Japan, 20 – 24 Apr. 2006.
 - [59] J. Whitmore, Talk presented at XIV International Workshop on Deep Inelastic Scattering (DIS2006), Tsukuba City, Japan, 20 – 24 Apr. 2006.
 - [60] For pp scattering without transverse polarization effects, which we consider here, the profile function depends only on the modulus of the transverse coordinate, $b = |\mathbf{b}|$. We nevertheless regard it as a function of the vector variable, \mathbf{b} , to facilitate later usage when we consider convolutions in the transverse coordinate variable.
 - [61] Notice that $1 - \Gamma(s, \mathbf{b})$ can be interpreted as the impact parameter representation of the S -matrix element, which is related to the scattering amplitude by Eqs. (64) and (65).
 - [62] In most of the recent literature the skewness is defined such that $2\xi = x' - x$. In the present context it is convenient to omit the factor 2 and define the skewness as in Eq. (16).
 - [63] In the present context it is convenient to define the gluon GPD as corresponding to the gluon momentum density, $xG(x)$, not the number density, $G(x)$, in the limit of zero momentum transfer.
 - [64] The Sudakov formfactor associated with the ggH vertex accounts for the absence of gluon bremsstrahlung with transverse momenta $|k_\perp| < |k_{\perp, \text{rad}}| < m_H/2$, radiated from the annihilating gluons. The requirement of absence of radiation from the screening gluon results in an additional shift of the k_\perp distribution towards larger values. However the amplitude for radiation from this line does not contain factors $\alpha_s \ln(k_\perp^2/m_H^2)$, and is beyond the accuracy of the calculation of Ref. [35].
 - [65] Note that the distribution $P_{\text{hard}}(\mathbf{b})$ of Eq. (75) (overlap integral of squared spatial distribution of gluons) is different from the distribution $P_4(\mathbf{b})$ (square of overlap integral of spatial distribution of gluons), which was introduced in Ref. [18] to describe double dijet production in inclusive high-energy $pp/\bar{p}p$ scattering. The two distributions coincide only in the case of an exponential parametrization of the two-gluon formfactor, which corresponds to a Gaussian dependence of the formfactors on transverse momenta and coordinates; see Eqs. (34) and (78). In general, it is not correct to replace $P_{\text{hard}}(\mathbf{b})$ by $P_4(\mathbf{b})$, as was done in Refs. [10, 11].
 - [66] The value $S^2 = 0.026$ quoted in Ref. [5] is obtained when taking into account corrections to the hard scattering amplitude resulting from the proton transverse momenta, which are not included in our approach. The difference between the two values is immaterial for the present discussion.
 - [67] It is worth noting here that diffraction in this case does not result from the presence of the fluctuations of the cross section strength. As a result, the cross section of diffraction is zero at $t = 0$. At the same time, the diffractive cross section ($dp \rightarrow pnp$) is not suppressed for $|t| \geq 1/R_d^2$, illustrating that diffraction cannot be described within the logic of the eigenstate scattering formalism [50, 51] for finite t . Also, there is no simple relation in this case between the Fourier transform of the diffractive amplitude (impact parameter representation) and the actual values of b in the process; the Fourier transform would suggest $\langle b^2 \rangle \propto 1/B$ [B is the slope of the pp elastic cross section, Eq. (5)], while in reality $\langle b^2 \rangle \propto R_d^2$.